Functional Connectivity Analysis of Visually Evoked ERPs for
Mild Cognitive Impairment

By
Lana Wang
May, 2022

Director of Thesis: Dr. Sunghan Kim
Major Department: Engineering

ABSTRACT

Mild cognitive impairment (MCI) is considered as the early stage of Alzheimer's disease, characterized as mild memory loss. Using electroencephalogram (EEG) data, a novel method of functional connectivity (FC) analysis can be used to detect MCI before memory is significantly impaired allowing for preventative measures to be taken. FC examines interactions between EEG channels to grant insight on underlying neural networks and can also allow for an examination of the effects of MCI on these neural networks. The FC method of weighted phase lag index (wPLI) provided insight on the link between the pathology of Alzheimer's disease and cognitive loss. wPLI was analyzed per frequency band (theta, alpha, mu, beta) and by channel combination groups (intra-hemispheric short, intra-hemispheric long, inter-hemispheric short, inter-hemispheric long, transverse). MCI was found to have a statistically significant lower $\Delta wPLI_{P300}$ compared to normal controls in the mu intra-hemispheric short ($p = 0.0286$), mu intra-hemispheric long ($p = 0.0477$), mu inter-hemispheric short ($p = 0.0018$) and the alpha intra-hemispheric short ($p = 0.0423$). Results indicate a possible deficiency in the dorsal visual processing pathway among MCI subjects as well as an unbalanced coordination between the two hemispheres.

Functional Connectivity Analysis of Visually Evoked ERPs for Mild Cognitive Impairment

A Thesis

Presented To the Faculty of the Department of Engineering

East Carolina University

In Partial Fulfillment of the Requirements for the Degree

MS Biomedical Engineering

by

Lana Wang

May, 2022

Functional Connectivity Analysis of Visually Evoked ERPs for

Mild Cognitive Impairment

By

Lana Wang

APPROVED BY:

Director of Thesis _____

Sunghan Kim, PhD

Committee Member _____

Brian Sylcott, PhD

Committee Member _____

Chris Mizelle, PhD

Chair of the Department of Engineering _____

Barbara Muller-Borer, PhD

Dean of the Graduate School _____

Paul J. Gemperline, PhD

Table of Contents

List of Tables

List of Figures

Chapter 1. Introduction

Dementia is a common condition that many elderly people experience, involving a loss of memory with Alzheimer's disease (AD) being the most common type of dementia. In the United States alone, more than 6 million people are living with Alzheimer's disease and the number is projected to rise to 13 million by 2050 [1]. Not only does dementia affect the lifestyle of the patient, but it also affects the patient's family in terms of providing care which is often extremely emotional. If dementia is detected at an early stage, various interventions can be made to slow down the progression of the disease. However, current testing methods, Montreal Cognitive Assessment (MoCa) and Mini Mental State Examination (MMSE), are not accurate where numerous false positives and false negatives are reported [2, 3]. There are numerous methods that some researchers have found success in detecting early onset of mild cognitive impairment (MCI), considered as the early stage of Alzheimer's disease, using time domain electroencephalogram (EEG) data. However, time-domain analysis is performed by analyzing EEG data at each individual electrode.

A new method has recently been introduced to the EEG community, called functional connectivity (FC). FC examines the interactions between EEG channels and therefore, the interactions of the underlying brain regions. FC provides holistic network-level information about how the different brain regions interact. By performing FC analysis on EEG data collected from MCI and AD patients, some researchers have been able to find FC differences that distinguish MCI/AD patients from healthy controls. However, all studies have been performed using resting state EEG data. This thesis proposes utilizing visually evoked event related potentials (ERP) data. ERPs are directly linked to cognitive processes such as memory and attention. Therefore, ERP data provides a better understanding of cognition compared to resting state EEG data. In theory, ERPs should

provide a better representation of the cognitive differences as well as provide better distinction between MCI and healthy subjects if analyzed via functional connectivity. FC analysis could act as a possible diagnostic method of MCI while also granting insight on connectivity strengths and patterns due to onset of dementia. FC analysis can also be implemented as a new standard of care for dementia patients, allowing for monitoring of dementia progression.

Chapter 2. Background

Dementia affects many people worldwide and is an umbrella term for symptoms related to cognitive declines such as memory loss and disorientation. Alzheimer's disease (AD) is the most common type of dementia, making up roughly 70% of dementia cases [4]. In the United States alone, more than 6 million people suffer from Alzheimer's disease and this count does not include other cases of dementia such as vascular dementia [1]. AD is characterized by the deterioration of cognitive abilities over time [4]. These patients are heavily impacted by memory loss leading to confusion, difficulties with visual images, misplacement of objects, and changes in personality [5]. Due to its irreversible and progressive nature, AD heavily impacts families. However, the disease can be caught early. There is a stage between healthy aging and AD referred to as mild cognitive impairment (MCI) [4]. MCI is marked by subtle cognition declines that do not directly interrupt daily life activities. A diagnosis of MCI does not necessarily mean that AD will develop, however, those with MCI have a higher turnover rate than the general healthy population. The conversion rates from MCI to AD can range from 4% to 31% [5]. Fig. 1 depicts the differences between dementia symptoms and typical age-related cognitive changes [6].

Signs of Alzheimer's and Dementia	Poor judgment and decision-making
Typical Age-Related Changes	Making a bad decision once in a while
Signs of Alzheimer's and Dementia	Inability to manage a budget
Typical Age-Related Changes	Missing a monthly payment
Signs of Alzheimer's and Dementia	Losing track of the date or the season
Typical Age-Related Changes	Forgetting which day it is and remembering it later
Signs of Alzheimer's and Dementia	Difficulty having a conversation
Typical Age-Related Changes	Sometimes forgetting which word to use
Signs of Alzheimer's and Dementia	Misplacing things and being unable to retrace steps to find them
Typical Age-Related Changes	Losing things from time to time

Figure 1: Differences between AD/Dementia symptoms and symptoms from normal aging [6].

Physiologically, AD is characterized by glucose hypometabolism. Glucose hypometabolism occurs due to a reduced activity of glucose transporters and reduced activity in enzymes that catalyze the breakdown of glucose [4]. Therefore, this leads to oxidative stress which further leads to a compromised blood brain barrier (BBB) and increased formation of amyloid-beta (Aβ) plaques and neurofibrillary tangles (NFT). Glucose hypometabolism is the start of AD pathology. However, glucose hypometabolism has not been well observed among MCI patients [4]. MCI patients have been found to show different patterns of hypometabolism localization, differing with each MCI patient [4].

Aβ deposit extracellularly while NFTs deposit intracellularly [7]. Aβs are formed after the amyloid precursor protein (APP) is cleaved by β and γ secretase [7, 8]. Formation of Aβs is normal, playing a role in attenuating oxidative stress [7]. In normal conditions, production and degradation rates of Aβ protein are in equilibrium [7]. However, in AD patients, there are deficiencies in enzymes causing a higher concentration of Aβ proteins [7]. There are deficiencies in degradation enzymes as well as mutations in γ secretase regulatory proteins [7, 8]. NFTs originate from microtubule originating tau proteins being hyperphosphorylated [9]. These hyperphosphorylated tau proteins aggregate intracellularly to form NFTs [9]. Protein aggregations also affect axonal transport and synapse disruption [9]. The combination of the compromised BBB and formation of Aβ plaques and NFTs further leads to neuron excitotoxicity and neuronal cell death [4].

Even though dementia is progressive, there are methods to slow down progression. Therefore, it is important to detect MCI prior to the onset of dementia. The earlier the disease is detected, the

higher the possibility is to preserve remaining cognitive by applying preventative measures. In particular, fasting and exercise have been found to enhance synaptic plasticity, neurogenesis, and cognitive performance [10] [11]. Exercise has shown to improve executive function, attention processing, memory, and learning [10]. Therefore, aerobic exercise lessens symptoms associated with AD [10]. These preventative methods can be set in place to slow down the progression of dementia.

2.1 Current diagnostic tests

There are two common tests for dementia: the Montreal Cognitive Assessment (MoCA) and the Mini-Mental State Examination (MMSE). These tests are the current standards in clinical settings to diagnose and assess MCI and AD. In multiple studies, MoCA has been found to be a more sensitive test for MCI and AD compared to the MMSE [2, 3]. The MoCA is divided into 7 sections: visuospatial/executive, naming, memory, attention, language, abstraction and orientation [2]. MoCA operates on a point system with 30 pts as the highest score, marked as healthy. Scores lower than 25/26 pts are considered to indicate a possibility of MCI. However, this cutoff is often changed in the research setting to promote higher sensitivity [2]. A sample MoCA test is attached in Appendix A.

The MoCA and MMSE tests have been examined for validity. In Parkinson disease patients, MoCA successfully diagnosed cognitive decline in 64% of people while MMSE correctly diagnosed 54% [2]. In this study, specificity for MoCA and MMSE were found to be 53% and 38% respectively [2]. In a separate study, MoCA correctly detected 100% of the MCI participants, however, 70.8% of healthy controls were labeled as MCI (specificity of 29.2%) [3]. When

checking for MoCA and MMSE validity, these tests do not perform well. This is due to the subjective nature of these tests, scoring of these tests are at the discretion of the clinician which varies. Aside from its subjective nature, these tests also have additional downsides. For example, in the MoCA test, the clinician would verbally read a list of words and the participant would repeat as many words as possible. This leaves room for vocabulary and language barriers causing a low MoCA score and a false positive. With these issues surrounding the MoCA and MMSE tests, many researchers are studying the use of other methods to detect MCI and AD using more quantifiable methods. The idea is not to eliminate these standard tests but to implement a better system at detecting MCI and AD by diminishing false positives and false negatives. An analogy to this scenario is asking a patient if they feel sick (MoCA) and taking a blood test (developing methods).

2.2 Technological methods

There are multiple methods to study brain functions, some invasive while others are not. Electrocorticography (ECoG) is an intracranial electrode where the electrodes are placed directly on the cerebral cortex to record the brain's electrical activity. Since these electrodes are intracranial, a surgeon must perform a craniotomy to expose the cerebral cortex. ECoG is a highly invasive measure to record brain activity, however, it has high signal to noise ratio and less susceptible to noise artifacts compared to non-invasive methods. Functional magnetic resonance imaging (fMRI) is a non-invasive method to evaluate brain function. fMRI does not pick up electrical activity but rather detects blood flow changes. Therefore, fMRI has high spatial resolution but low temporal resolution as data is not collected continuously throughout a session. Another common non-invasive method is called electroencephalogram (EEG). EEG electrodes are worn as a cap, placed on the scalp. These electrodes pick up electrical activity on the scalp, and

are thought to be representative of the brain's electrical activity. In contrast to ECoG, EEG has a low signal to noise ratio. Between the electrode and the brain, there are multiple layers the electrical signal has to pass through such as the skull. Therefore, this causes the recorded electrical signals to be extremely weak. EEG electrodes will also pick up other physiological signals as well as eye movements signals (EOG) and electromyography (EMG) signals. EEG signals are collected continuously over time granting high temporal resolution and is often the desired method of data collection for many researchers due to versatility and high temporal resolution. When studying cognition, temporal resolution is desired to determine if certain health conditions such as AD/MCI affect reaction speed.

2.3 EEG source

The source of EEG signals arises from post-synaptic potentials from pyramidal neurons along the cortical columns [12]. When these post-synaptic pyramidal neurons are excited, the dendrites become more negative than the body of the neuron [12]. The imbalanced distribution of the extracellular voltage creates dipoles [12]. When the EEG channels pick up signals, it is picking up a sum of the positive and negative charges in its vicinity [12]. Since it is picking up the sum of charges, the underlying neurons need to have a synchronized activity to yield a net charge and not cancel the charges [12]. If the charges cancel out, the EEG channel will not pick up any signal. The sum of all the neuronal charges in that respective EEG channel area is treated as a single dipole in post-processing analysis [12]. EEG signals picked up in relation to the pyramidal neuron's charge distribution is depicted in Fig. 2 [12]. In areas of negative extracellular voltage, the EEG channel will pick up a negative potential and vice versa. As stated before, these electrical signals have to travel through multiple layers of tissue to finally be picked up by an EEG electrode. The

neuronal signals have to travel from the brain through dura layers, skull layers, and the scalp where it will finally be picked up by the electrode [12].

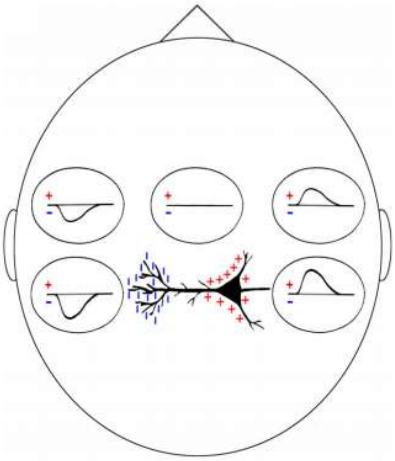

Figure 2: Recorded EEG based on neuronal dipoles, an example [12].

There is a standard for EEG electrode placement known as the 10-20 international system, illustrated in Fig. 3. This system indicates where electrodes should be placed and its corresponding name. The electrodes are named based on the location and the specific brain lobe that it covers. Electrodes are named as lobe location followed by a number, i.e. F3. The four lobes are abbreviated as follows: occipital (O#), parietal (P#), temporal (T#), and frontal (F#). Along the middle horizontal line, electrodes are named as C#. Electrodes lying in the "middle" of the lobes are named accordingly, i.e. CP# for central parietal. Electrodes on the midline (center vertical line) are labeled using the lobe abbreviation followed by "z". The right hemispheric electrodes are numbered by even numbers while the left hemispheric electrodes are numbered by odd numbers.

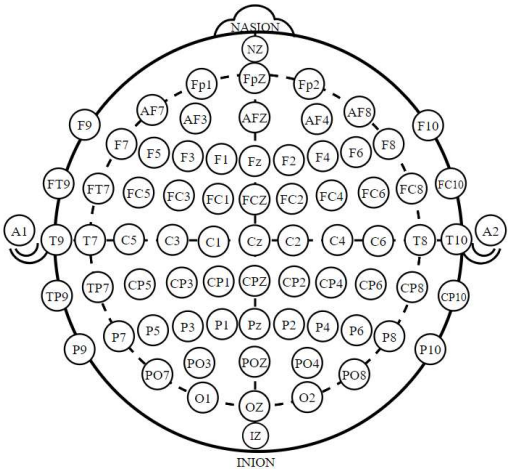

Figure 3: 10-20 international system for EEG electrode placement [13].

2.4 Event Related Potentials and Time Domain Analysis

To study cognition, researchers often opt for stimulus presentation either visual or auditory. Data collection involves presenting multiple sets of stimuli. However, there are specific target stimuli that are presented in random and are recognized by the participants. Known as the odd ball paradigm, these target stimuli will elicit stronger brain activity as they are presented randomly and are familiar to the participants. For example, visual stimuli can involve generic faces with target stimuli being a famous actor. This famous actor stimuli will be presented at random and due to familiarity, will result in stronger brain activity. To present these visual stimuli to participants, a software known as BCI2000 is often used. BCI2000 allows for real time data acquisition, and processing. In particular, BCI2000 is used to determine the presentation algorithm, i.e. how long to present the images, how often images are presented, and time in between image presentations. BCI2000 will present each image in a random order to adhere to the odd ball paradigm.

On an EEG standpoint, the stimulus presentation triggers the brain resulting in an elicited event related potential (ERP). An ERP is time-locked to the specific stimulus and is thought to reflect the participant's cognitive ability. Different components of an ERP have been found to be associated with different cognitive functions. The most studied ERP component is the P300, a positive deflection occurring at around 300ms after stimulus presentation. The P300 component is correlated to attention and cognitive decline where these factors affect the P300 characteristics [14]. Furthermore, the P300 can be divided into the P3a and the P3b. The P3a is associated with attention and stimulus processing while the P3b is associated with decision making [14]. This particular ERP component, P300, has been studied with both visual and auditory stimuli [14] [15].

Time-domain analysis directly utilizes these ERP components, where the ERP components can be broken down to determine its amplitude and latency, both determined at the ERP component's highest point of deflection. Amplitude reflects how actively the brain responds while latency reflects how quickly the brain reacts to a stimulus. Both MCI and AD have been found to affect P300 latency compared to healthy controls with statistically significant prolonged latency [14] [16] [17]. Additionally, it has been found that the P300 latency increases as the disease progresses from MCI to AD [14] [16] [17]. Aside from latency, some studies have reported diminished P300 amplitudes while some have not. In a study by van Deursen et al, AD subjects had statistically significant lower P300 amplitudes compared to healthy controls at electrodes Cz and Pz [16]. Newsome et al found significantly reduced P300 data between at-risk subjects and healthy controls in the Fz and Cz channels [15].

While time-domain analysis is important and informative, there are many more methods to study EEG data that are much more interesting and grant further information that time-domain results will not portray. One such method that is becoming increasingly more popular is called functional connectivity. Time-domain analysis, studying ERPs over time, provides localized information at each collecting EEG electrode. When analyzing time-domain EEG data, the analysis takes place electrode by electrode, i.e. P300 amplitude at electrode Cz is diminished. On the other hand, functional connectivity (FC) evaluates if and how neuronal activity in one region of the brain relates to neuronal activity in another region [18]. Therefore, by studying the interactions between EEG channels, FC grants holistic information that could not be captured by traditional time-domain analysis. Relatively new to the EEG community, FC has been successfully and commonly used in the fMRI community [18]. The benefit of this method to EEG studies is being able to evaluate FC in millisecond increments that cannot be captured in high resolution using fMRI data.

2.5 Functional Connectivity

With EEG data, functional connectivity studies the degree of synchronization between the EEG electrodes to evaluate the brain's network level activities. Functional connectivity is analyzed per frequency band, and therefore, analysis is dependent on the frequency domain. Therefore, it requires the use of some transformation that allows for extracting of frequency information from EEG signals.

FC evaluates simultaneously recorded EEG signals to examine the degree of synchronous activities of different brain regions, which are statistically significant [19]. The overall hypothesis is that neuronal oscillations and their respective synchronization reflect underlying dynamic

coordination within the brain [20]. The brain is thought to dynamically coordinate information flow by adjusting strength, pattern, or the frequency causing brain regions to engage in neuronal oscillatory synchronization [20]. Specifically, when studying functional connectivity, calculations are performed to look at bivariate networks, i.e. examine two channel's coupling at one time. The brain operates on multivariate networks where multiple areas of the brain are involved in the brain network, however, this is difficult to computationally calculate [19]. Therefore, when analyzing bivariate networks, there could be multivariate reasoning behind the findings. Functional connectivity is also calculated as acausal networks, meaning the EEG channel signals indicate that the areas are coupled together to fulfill one function [19]. However, in reality, connectivity is causal meaning one area is stimulating another area to fulfill the function [19]. There are some FC methods that study causal networks; however, it heavily relies on the accuracy of the multivariate autoregressive models used in the calculations [19]. These models are difficult to validate as there is no method to test if these models are accurate representations of the neuronal dynamics observed in the brain. The only way these models are considered "accurate" is from conceptual understandings and assumptions regarding these brain dynamics. There are already numerous assumptions underlying each FC method and methods that study causal networks add yet another assumption by incorporating the autoregressive models.

With functional connectivity, there are also volume conducting effects. EEG electrodes are placed all along the scalp. Therefore, when one area of the brain becomes active, this electrical activity is hypothetically being picked up on all the electrodes. Electrodes further from the active area pick up weaker signals while closer electrodes pick up stronger signals. These volume conducting effects aid in determining the 3D location of brain activity. However, for functional connectivity,

volume conduction effects can cause data bias [18]. Two EEG channels can be computationally calculated as functionally connected (coupled), however, they could have just picked up the same signal. In these cases, these channels are artificially connected, i.e. connected due to volume conduction but in reality, are not functionally connected [18]. Early FC methods such as coherence have been criticized as it does not factor in volume conduction effects. More FC methods have been developed subsequently to eliminate or minimize the effect of volume conduction. There are numerous methods that have been proposed, Wang et. al evaluated 42 different methods with each having their own advantages and disadvantages [20] [21].

2.5.1 Cross-correlation

In 1951, early forms of FC were studied using cross-correlation to study EEG signal similarities [22][23]. The correlation method measures linear connectivity based on the Pearson's coefficient by analyzing signal similarity linearly [20]. Cross-correlation is calculated by sliding one signal over the other signal and multiplying the two signals at each point as depicted in Fig. 4. A major downside of the correlation method is that it ignores the temporal structure of the signals and treats each data point as random variables [20]. Therefore, cross-correlation has to be evaluated as a function of time lag to factor in the temporal nature of EEG data [20]. Cross-correlation is sensitive to both phase and polarity information and its values ranges from -1 to 1 [22]. This method has been effective to study neuronal networks that exhibit unidirectional interactions with maximum correlation at a specific time lag [20]. However, studying bivariate interactions becomes tricky and difficult to analyze [20].

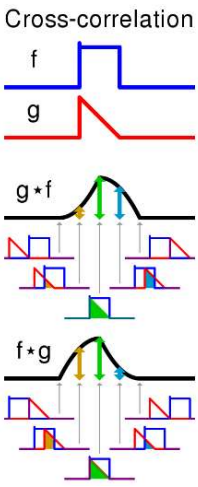

Figure 4: Illustration of cross-correlation calculation given two example signals, f and g [24].

2.5.2 Coherence

Coherence is another one of the first FC methods adopted in the EEG community dating as early as the 1960's [25]. Coherence is based on statistical theory of stochastic processes [20]. It is defined as the spectral correlation between two EEG time series which mathematically is the frequency domain equivalent to time-domain cross-correlation function therefore, it also measures linear connectivity [26] [20]. The idea of coherence is to evaluate if two signals can be related using a linear time invariant transformation meaning a constant amplitude and phase difference over time [27]. Coherence values range from 0 to 1 due to the normalization from the individual power spectra [20]. A coherence coefficient of 1 at a given frequency indicates that the power in one signal can be predicted by the power in the other signal at that given frequency [26].

Overall, coherence is sensitive to both power and phase with a loss of polarity information while assuming that underlying neural dynamics are linear [22][27]. Coherence and correlation both determine if the two signals can be statistically represented by a linear function (i.e., the Pearson's

coefficient). A major limitation to coherence is its prime contamination to volume conduction effects, this method has no system in place to eliminate or diminish volume conduction [27]. With simulated uncorrelated dipole sources, coherence measured substantial effects due to volume conduction between two EEG channels if the electrodes were separated by less than 10cm [27]. As the distance between the two EEG channels decreases, volume conduction effects become larger [27]. Electrodes separated by more than 20cm still exhibited small volume conduction effects [27]. Coherence's sensitivity to volume conduction has been observed by numerous researchers [28, 29, 30].

2.5.3 Phase locking value

Lachaux et. al first introduced the functional connectivity method of phase locking value (PLV) in 1999 [31]. PLV is one of the first methods developed that evaluates signal coupling as a non-linear method. Non-linear functional connectivity methods were developed due to findings of neural processes that contain non-linear characteristics such as the regulation of the voltage-gated ions [19]. Coherence and correlation both measure if two EEG channels are linearly correlated, non-linear methods do not place the assumption that neural dynamics can only be represented linearly. PLV is based on the idea that functionally connected brain regions will produce signals that will have instantaneous phases evolving together (i.e. phase locked) [32]. A major assumption to phase synchronization FC methods is that dynamic neuronal systems will have their phases synchronized when their amplitudes are not correlated [19]. Therefore, this method ignores signal amplitudes and is focused directly onto phase differences. To calculate PLV, the first step is to obtain the instantaneous phase of each signal using Hilbert Transform or a wavelet transform such as Morlet [32]. The benefit of using the Morlet wavelet transform is it allows for narrow-band pass filtering

convolution so that only one oscillator is present in each signal [32]. PLV evaluates the mean phase differences between two signals over trials, n, at a defined time point, t [31]. These instantaneous phases of two channels, $\theta_1(t,n)$ & $\theta_2(t,n)$, are used to calculate PLV using Equation 2 [31]. PLV ranges from 0 (no phase dependence) to 1 (phase dependence) [31, 32, 33]. Even with the new development of the PLV method, this method is also not immune to volume conduction effects [33].

$$PLV = \frac{1}{N}\left|\sum_{n=1}^{N} e^{j(\theta_1(t,n)-\theta_2(t,n))}\right| \quad (2)$$

2.5.4 Phase Lag Index

The use of phase lag index (PLI) is another method to study functional connectivity proposed by Stam et al. in 2007 [28]. One primary difference is that PLI introduced the concept to discard phase differences that are centered around 0 mod π to completely eliminate volume conduction effects [28]. When defining an asymmetry index for phase differences distribution while centered around zero, if there is not a presence of phase coupling, there will be a flat distribution [28]. Indication of phase synchronization occurs when there is any deviation from a flat distribution [28]. Between two signals, the phase difference is measured at each time point through the imaginary component of the cross-spectrum. When these phase differences are portrayed on the complex plane as depicted in Fig. 5, phase differences lying on 0 mod π (purple and orange lines) are discarded (i.e. the flat distribution stated by Stam et al). The reason behind discarding these phase differences is due to volume conduction. If volume conduction is playing an effect on the measured EEG signals, the signals would have a phase difference of 0 or they would have a phase difference of π. A phase

difference centered around 0 would be observed since the signal is emitted by one singular source and measured by multiple channels. A phase difference centered around π would be observed also by signal emission by one source, however, the signal is being picked up by channels in opposite directions. While a phase difference of 0 mod π is being discarded, there is a possibility that these phase differences are derived from a true functional connectivity between brain regions [28]. The PLI method eliminates possible volume conduction effects while also possibly eliminating a true strong connectivity between signals, i.e. EEG channels. When a phase outside of 0 mod π is observed (green lines in Fig. 5), the idea is that this could not be due to volume conduction and must be due to true phase synchronization [28].

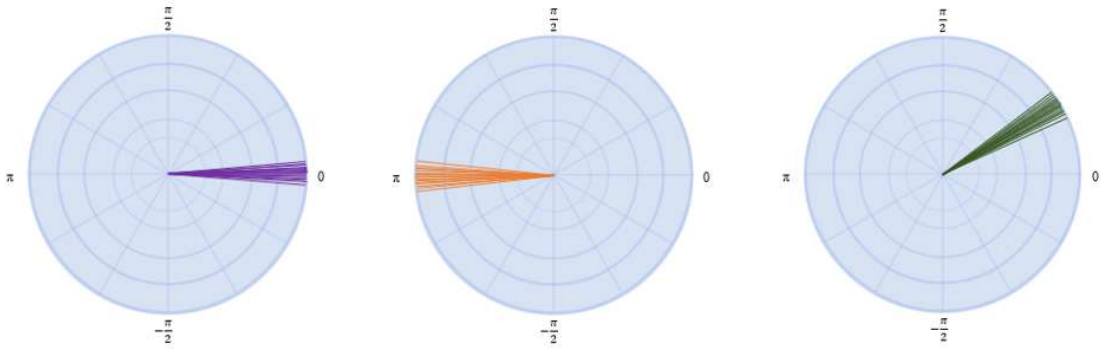

Figure 5: Phase differences portrayed on the complex plane indicating discarded phase differences (purple and orange) and phase differences that are considered valid (green).

Measured phase differences can then be converted to a PLI value. A generalized phase lag index calculation can be seen in Equation 3 where Δϕ(tk) is a time series of phase differences [28].

$$PLI = |\langle sign[\Delta\phi(t_k)]\rangle| \quad (3)$$

A more detailed calculation for PLI can be seen in Equation 4. PLI is calculated among multiple trials, n at a designated time, t. When looking at the phase difference, only the complex, imaginary component is of interest, $\Im$. Therefore, the PLI value at one trial and at one time can only be -1 or 1. The overall PLI value is calculated by averaging the PLI values among all the trials which the absolute value will yield phase lag index values ranging between 0 and 1 [28]. PLI of 0 indicates no coupling and a value of 1 indicates perfect phase locking [28]. The stronger the phase locking, the larger the phase lag index value will be [28]. Based on this equation, it cannot be determined if one signal is leading or lagging another signal, however, by eliminating the absolute value, this information can be determined [28].

$$\begin{aligned} \text{PLI} &= |E\{sign(\Im(X))\}| \\ &= \left|\frac{1}{N}\sum_{n=1}^{N} sign(\Im[e^{j(\Delta\phi)t}])\right| \end{aligned} \tag{4}$$

Stam et al. utilized the Kuramoto Model with 64 simulated oscillators to test the effectiveness of the PLI method in comparison to imaginary coherence [28]. The model was adjusted to various strengths of coupling where PLI was more sensitive to coupling strength when compared to the imaginary coherence [28]. With these models, Stam et. al simulated volume conduction by applying common sources [28]. Both methods show a decrease in FC values as common sources increase [28]. Fig. 6 illustrates the responses by the PLI and imaginary coherence methods due to changes in coupling strength and by common sources [28].

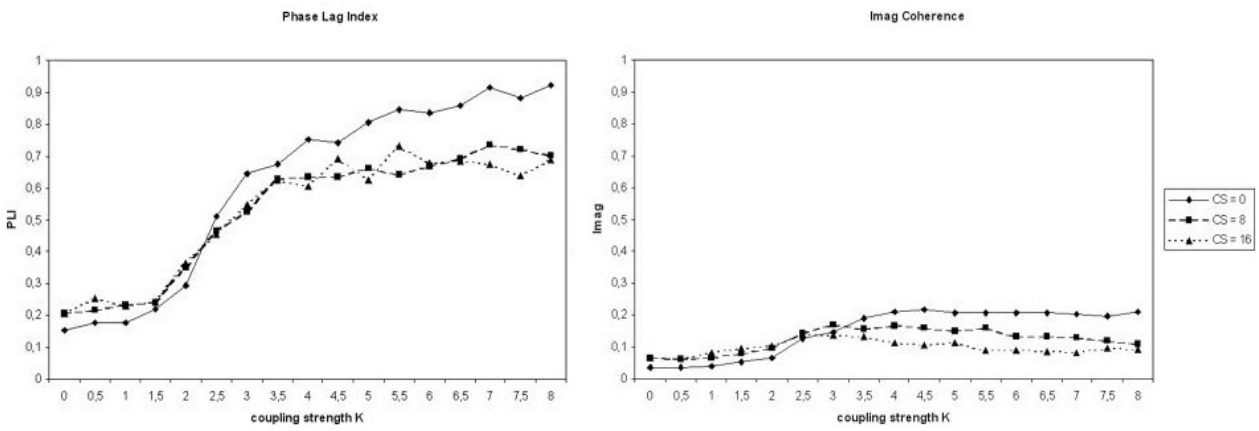

Figure 6: PLI and ICoh values based on simulated oscillators as a function of coupling strength and common sources (volume conduction) [28].

2.5.5 Weighted Phase Lag Index

In recent articles, it has been found that phase lag index's sensitivity to volume conduction is hindered by the discontinuity within the measurement [34]. This causes a problem for phase synchronization of small magnitudes where the small perturbations turn phase leads into lags [34]. Therefore, a new method to analyze phase synchronization was proposed in 2011 called the weighted phase-lag index [34]. The weighted phase-lag index is obtained by calculating the cross-spectra's imaginary components, $\Im\{X\}$, and weights the contribution of the phase leads and lags by the imaginary component's magnitude [34]. The equation for wPLI can be seen in Equation 5.

$$wPLI = \frac{|E\{|\Im\{X\}|sign(\Im\{X\})\}|}{E\{|\Im\{X\}|\}} \tag{5}$$

With wPLI, the normalization limits, not eliminates, the influence of small noise perturbations causing the cross-spectrum to rotate across the real axis, changing phase leads into lags [34, 35].

The noise can cause the cross-spectrum to calculate a phase lag when it is actually a phase lead. PLI calculations exacerbate the effects of the noise due to only capturing the sign of the phase, i.e. +1 or -1 [34]. However, wPLI normalizes the sign by the magnitude of the imaginary component and minimizes the effect of the noise [34]. Therefore, a larger magnitude of the imaginary component (larger phase difference) causes the wPLI value to become smaller and a smaller imaginary component (smaller phase difference) causes the wPLI value to become larger. The numerator for the wPLI calculation allows for distinguishing between a phase lead and a phase lag. Fig. 7 provides a visual as to how the weighting of the wPLI distribution is different compared to PLI [34].

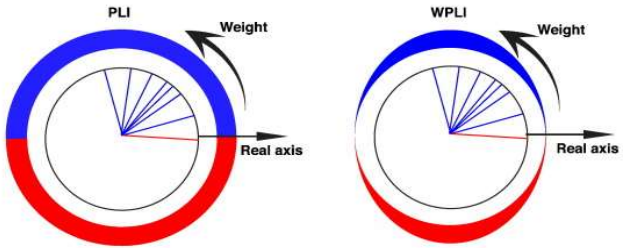

Figure 7: Differences between PLI and wPLI distribution due to wPLI's application of a weighting [34].

Since both methods, i.e. phase lag index and weighted phase lag index, are relatively new, both methods are still actively used in this field. There does not seem to be an agreement in this field regarding which method is better to analyze phase synchronization. However, wPLI seems to be more sensitive to phase differences due to their application of weighting. In literature, more researchers tend to use wPLI as opposed to PLI.

2.5.6 Functional connectivity summary

Even though all three phase synchronization methods utilize the phase difference in calculations, there are distinct differences in the way the phase differences are calculated. Given the cross-spectrum output at a specific frequency to be 1+2i, these methods will calculate phase differences according to their own respective method. PLV will calculate the phase given both real and imaginary component through $\theta = \tan^{-1}(2/1)$. Due to this calculation, the PLV method is blind to changes in overall magnitude, a cross-spectrum output of 2+4i will give the same phase angle and 0.5+1i will also give the same phase angle. PLI will only grab the sign of the imaginary component, since the imaginary component is 2i then the sign would be +1. Therefore, this calculation isn't truly grabbing amplitude or phase differences. wPLI also only utilizes the imaginary component but will grab both the sign and magnitude of the imaginary component. By grabbing the imaginary component's magnitude, wPLI overcomes the PLV's downside of ignoring overall magnitude changes. Fig. 8 summarizes the differences between the phase synchronization methods discussed.

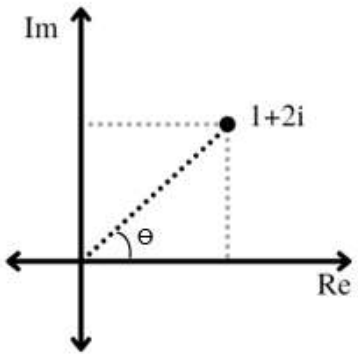

FC Method	Phase difference
Phase locking value	Grabs Θ, blind to overall magnitude similarities, ex. complex number of 2+4i would give the same phase angle
Phase lag index	Grabs the sign of the imaginary component, ex. +1
Weighted phase lag index	Grabs magnitude of imaginary component and grabs the sign of the imaginary component

Figure 8: Differences between the 3 phase synchronization methods based on calculations and how the methods determine phase differences between two vectors.

In general, it is difficult to validate any of these methods, as there is no way to actually determine if these methods accurately describe the functional connectivity of the brain. Researchers have simulated coupled oscillators to test different FC methods for accuracy, however, these simulated oscillators are not a direct representation of the brain. FC methods are used to try to understand how the brain communicates, there is not a current validated method/model that FC can be compared to for accuracy and effectiveness. Therefore, these FC methods are checked for "accuracy" by conceptual understanding. For example, cross-correlation and coherence are not considered accurate by the EEG community because the brain's neuronal dynamics are most likely not linear. To the EEG community, it makes more sense that brain regions are functionally connected by phase rather than by amplitude.

2.6 EEG Frequency bands

Functional connectivity is often calculated and determined based on the EEG frequency bands. There are seven frequency bands: delta (1-4Hz), theta (4-8Hz), alpha1 (8-10Hz), alpha2 (10-13Hz), mu (8-12 Hz), beta1 (13-18Hz), and beta2 (18-30Hz) [35, 36]. Some researchers will combine the alpha sub-bands and beta sub-bands, i.e. without separating alpha band into two separate bands.

The delta band is most commonly associated with the P300 ERP, where the P300 amplitude positively correlates with delta band power [37]. Given that the P300 correlates with working memory, attention, and motivation (satisfy basic needs), the delta band is assumed to correlate with these three psychological processes [37]. The theta oscillations are thought to be involved with multiple behavioral, cognitive and emotional processes such as involvement in the encoding

of information [37]. Theta also has high involvement with the P300 and can also be assumed to be involved in salience detection, a key attentional mechanism [37]. Alpha oscillations are strongly thought to correlate with memory operations as well as inhibitory processes (i.e. occipital-parietal area becomes inhibited to suppress input from other areas) [37]. Mu rhythm is a special subset of alpha, and is thought to be representative of sensorimotor, where mu will suppress with movement execution [35]. Classification of mu as a frequency range differs among research studies, however, the frequency range always overlaps with the alpha band. The beta band has been found to be associated with attentional modulation [38]. When the elderly are compared to young adults, they tend to show a decrease in beta-band activity compared to young adults reflecting difficulty in activation of attentional processes [38].

With these frequency bands, the community does not have a consensus with which psychological processes the specific bands correlate to and the community does not know exactly how the bands correlate to the psychological processes. For example, the community does not know exactly how the beta band correlates with attention modulation. A summary of the frequency bands and its correlated psychological processes can be seen in Table 1. However, since the subject population of interest is MCI, the frequency bands of interest are theta, alpha, mu (upper alpha), and beta. These frequency bands are most commonly known to be associated with attention and memory, processes that pertain to dementia.

Table 1: Summary of each frequency band and their corresponding psychological process based on literature assumptions and studies.

Frequency Band	Psychological Processes
Delta	Behavioral, cognitive, and emotional Encoding of information
Theta	Attention
Alpha	Memory processes
Mu	Sensorimotor
Beta	Attentional modulation

2.7 FC and Alzheimer's Disease

Functional connectivity has been evaluated among the Alzheimer's and MCI population, however, there are not that many articles as of now that have been published using the newer FC methods of PLI and wPLI. In numerous studies, and in all studies mentioned in this proposal, EEG was recorded at resting state. Therefore, subjects were seated with eyes closed, in wakefulness state while remaining stationary.

Through coherence studies, significant differences between AD and healthy controls have been found among multiple frequency bands. In one article, researchers found significant decreases in FC observed from AD subjects in all frequency bands from theta to upper beta when utilizing the coherence method [26]. The majority of the functional connectivity differences between the subject groups were found in the frontal and central regions [26]. Another study detected differences using the imaginary coherence method where the average IC value for AD patients was significantly lower overall compared to healthy controls ($p = 0.002$) in the 13-30 Hz (beta) frequency band [28]. IC values were also divided into 4 different groups and further averaged: (1)

intra-hemispheric short; (2) intra-hemispheric long; (3) inter-hemispheric short; (4) inter-hemispheric long [28]. AD patients also showcased a lower IC in the short intra-hemispheric distances (p=0.005) and in the long inter-hemispheric distances (p=0.013) [28].

When Stam et. al compared AD and controls using IC, these researchers also evaluated FC differences by measuring PLI values in the beta band. Using the overall averaged PLI values, AD had significantly lower PLI values compared to controls (p=0.009) in the beta band [28]. AD also had lower PLI values in the short intra-hemispheric distances (p=0.032) and in the long intra-hemispheric distances (p=0.016) [28]. Fig. 9 shows the results from Stam et al. from the IC and PLI methods [28].

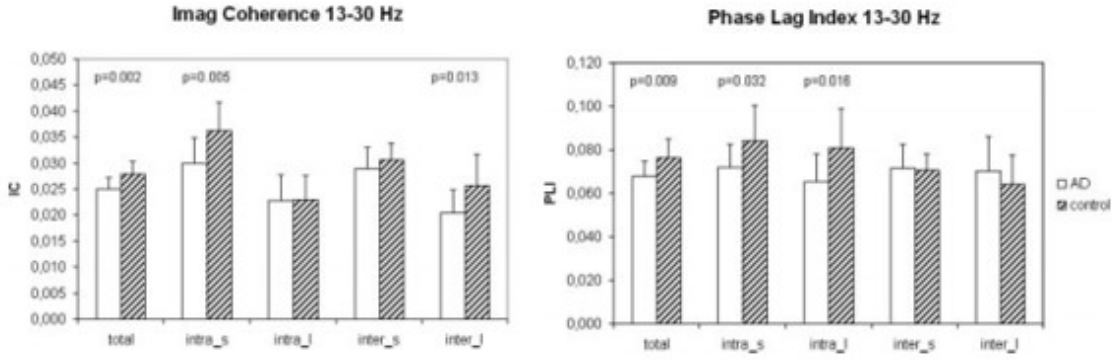

Figure 9: Comparing AD and healthy controls using both the ICoh and PLI methods [28].

Briels et al also compared multiple FC methods (coherence, imaginary coherence, PLV, PLI, and wPLI) as well as tested these methods for reproducibility. The subject pool included AD subjects and those with subjective cognitive decline (SCD) [39]. Coherence detected a lower functional connectivity from the AD subjects in alpha and beta bands [39]. PLV only detected functional connectivity differences in the alpha band with AD subjects presenting lower connectivity

compared to SCD subjects [39]. Imaginary coherence, PLI and wPLI showed a higher functional connectivity in the theta band among the AD subjects [39]. Briels et al summarized their findings using the Cohen's d statistical method of determining effects size where a d=1 indicates that the AD subjects differ from SCD subjects in FC values by 1 standard deviation [39]. Fig. 10 illustrates the calculated Cohen's d for coherence, imaginary coherence, PLV, PLI and wPLI as well as two other FC methods that were not discussed in this proposal (amplitude envelope correlation (AEC) and corrected amplitude envelope correlation (AEC-c)) [39]. To evaluate reproducibility, AD and subjective cognitive decline (SCD) subjects were randomly divided into 2 cohorts [39]. FC methods were analyzed in each cohort separately and results were compared to each other [39]. Based on this analysis, PLI and wPLI showed reproducibility in the alpha band [39].

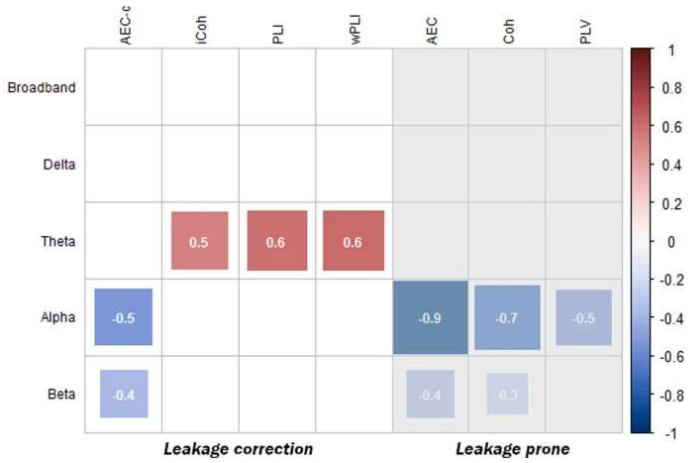

Figure 10: Comparison between multiple FC methods at distinguishing between AD and SCD subjects by using the Cohen's d statistical method [39].

In a separate study, AD was also differentiated from controls using the PLI method [40]. Kasakawa et al. visually illustrated PLI values over a specific threshold of 0.1, as seen in Fig. 11. With these images, the subject groups differ in FC among the frequency bands. AD subjects tend to have higher FC on the lower frequency bands where little connectivity is seen in the higher frequency

bands, and vice versa for the healthy controls (HC) [40]. However, these researchers did not report the actual strength of these PLI values.

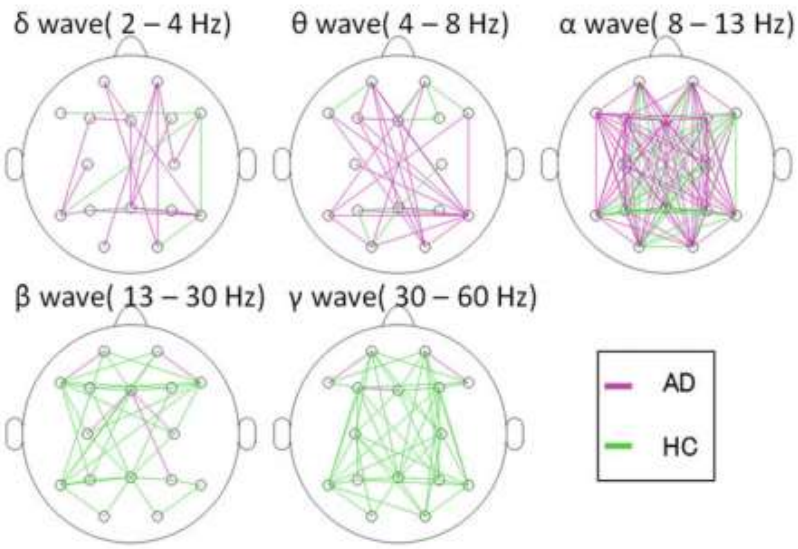

Figure 11: Illustration of PLI functional connectivity of AD and healthy controls across the multiple frequency bands where threshold was set at 0.1 [40].

With AD and MCI patients, studies have also been performed that directly look at different EEG frequency bands in methods aside from traditional FC. Koenig et al studied numerous subjects with different degrees of cognitive impairment (MCI, mild-severe AD, etc.) utilizing global field synchronization (GFS, a method developed by these researchers). GFS statistically significantly decreased at a statistically significant rate as cognition worsened in the alpha and beta bands as illustrated in Fig. 12 [41]. The decrease in GFS is most pronounced in the alpha band but still clearly seen in beta [41]. Interestingly, severe AD patients had a significant increase in GFS in the delta band, possibly due to the brain anatomy differences in severe AD [41]. Certain therapies with acetylcholinesterase inhibitors have shown to cause an increase in delta and theta activity [41]. A decline in gamma band GFS is also observed, however, it was not statistically significant [41].

Through a different study involving MEG data rather than EEG data, the findings supported the decrease in synchronization [42]. This study used the synchronization likelihood method (also not discussed in this proposal) and found synchronization in AD patients to be lower in the upper alpha band (10-14Hz, p=0.016), upper beta band (18-22Hz, p=0.037) and the gamma band (22-40Hz, p=0.033) [42]. When evaluating differences when using coherence, no statistical differences were found between AD and healthy controls [42]. In contrast, van Deursen et. al found an increase in EEG gamma activity among AD patients when compared to MCI and healthy controls. However, there was no difference between the MCI and healthy controls [43].

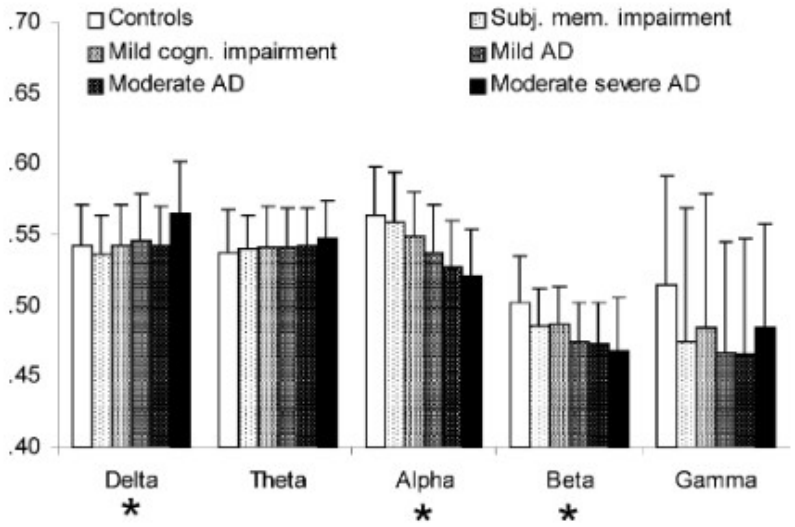

Figure 12: Comparison between multiple degrees of dementia ranging from healthy controls to moderate severe AD by utilizing the GFS method [41].

Studies have also examined differences between AD, MCI and healthy subjects purely on the power observed in the frequency bands with EEG data. Fig. 13 illustrates differences detected among multiple frequency bands between AD, vascular dementia (VaD), and healthy controls (Nold) [44]. AD subjects had a significant reduction in alpha 2 (9-11 Hz) and alpha 3 (11-13Hz) power when compared to controls and significant reduction in alpha 2 power compared to VaD

subjects [44]. In both AD and VaD subjects, the delta band (3-5 Hz) power was significantly increased compared to controls [44]. In a separate study by Moretti et. al, progressing MCI subjects were found to have a high EEG alpha 3-alpha 2 power ratio which was found to be associated with temporo-parietal cortical thinking and memory impairment [45].

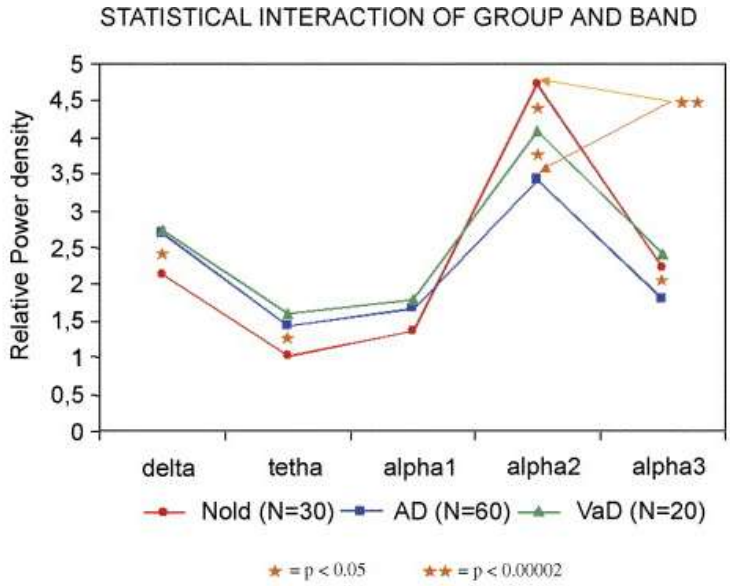

Figure 13: Frequency band power differences between healthy controls, vascular dementia (VaD), and Alheimer's disease (AD) subjects across multiple frequency bands [45].

In general, none of the FC methods contradicted each other aside from coherence. However, some FC methods would detect differences in FC while some would not detect connectivity differences. Connectivity differences between AD and healthy controls were observed in frequency bands of theta to gamma where only a power difference has been observed in the delta band. Table 2 summarizes the FC findings among AD patients; however, few studies have been performed thus far. Conceptually, MCI and AD patients would show decreased FC due to attentional deficits and memory deficits. Therefore, an increase in delta and theta band is surprising. Only severe AD

patients were observed to have increases in delta and theta, this observation was not noticed among the MCI population [40, 42].

Table 2: Summary of FC and power differences when AD is compared to healthy controls based on numerous research articles.

Frequency bands	**AD/MCI compared to healthy controls**
Delta (1-4 Hz)	Increased power
Theta (4-8 Hz)	Increased FC, decreased coherence, increased power
Alpha (8-13Hz)	Decreased FC, decreased coherence, decreased power
Beta (13-30 Hz)	Decreased FC
Gamma (30-45 Hz)	Decreased FC, Increased activity

Chapter 3. Thesis Hypothesis and Significance

MCI subjects have been found to have FC differences compared to healthy subjects, however, it has not been thoroughly studied with few studies being performed thus far. All these studies involved using resting EEG data, however, by using ERP data, MCI subjects could show a larger FC difference compared to controls. Time domain ERPs have been associated with cognition, so frequency domain analysis of ERPs through FC should correlate with cognition better than resting state EEG data. These ERPs are generated using familiar face visual stimuli. The hypothesis is stated as below:

> **The hypothesis is MCI patients will show decreased FC using the wPLI method in all frequency bands (theta, alpha, mu/upper alpha and beta) by using familiar face ERP data when compared to healthy controls.**

In this study, the P300 will be studied, and it is hypothesized that the wPLI results will indicate lower FC in MCI subjects. Conceptually and based on symptoms, MCI patients tend to have a more difficult time recognizing faces and therefore, should elicit a worsened P300 either by amplitude or latency. It is hypothesized that wPLI results will reflect the decreased ability in facial recognition and memory retrieval that is commonly found using time-domain analysis.

In the hypothesis, the wPLI results are expected to be lower in MCI subjects in all frequency bands. This somewhat contradicts prior research with these subject groups. With resting state EEG FC analysis, prior researchers have found increased FC in the delta and theta bands in patients with severe AD. In this study, MCI subjects are being studied instead of AD, therefore, the increase in

FC in the lower frequency bands is not expected. Physiological changes in AD are not necessarily observed among MCI patients (hypometabolism, protein aggregation) and therefore, can be difficult to use previous AD FC research as a predictor for MCI FC.

The purpose of this study is not to pursue a replacement to the MoCA or MMSE tests but to pursue a supporting test to detect MCI. MCI has been analyzed primarily by time-domain analysis, which only give channel by channel information whereas FC gives holistic information. By analyzing FC, holistic information, of MCI subjects, the results can also grant insight on differences in connectivity pathways. Physiologically, AD patients showcase hypometabolism and protein aggregation leading to worsen signal propagation and neuronal cell death. Therefore, this raises the possibility that MCI and AD patients utilize different neural pathways to complete a cognitive function. MCI and healthy subjects may have completely different functional connectivity, i.e. different brain interactions. Therefore, finding these differences may provide more insight as to how MCI patients process visual information differently.

MCI often leads to developing AD, a crippling disease. In some cases of severe AD, the patient will forget their identity and forget the identities of their family. The disease not only affects the patient but heavily impacts the family as well. There have been therapies found that can slow down progression of dementia. If MCI is diagnosed early, development into AD can be slowed causing an improvement in quality of life. At the very least, the patient and their family can prepare for the onset of AD.

Chapter 4. Methods

There are many steps needed to analyze data and prove or disprove the hypothesis. These steps range from data collection to data processing to statistical analyses. In this thesis, data processing involves numerous steps to consolidate data to form data structures allowing for further analysis.

4.1 Data Collection

Data collection was composed of two tests: a MoCA test and EEG collection where collection was performed in 2018 and 2019 at the Greenville senior center, Ayden senior center, Bethel senior center and Farmville senior center with a total of 38 subjects. A trained professional administered the MoCA test to each participant before EEG data was collected. To collect EEG data, the participants were seated five feet away from a 42" LED television. Data was then recorded from an electrode cap containing 16 dry gold-plated g®.SAHARA EEG electrodes. Electrodes were placed based on the 10-20 international system at locations: FPz, F7, F3, Fz, F4, F8, C3, Cz, C4, P7, P3, Pz, P4, P8, O1, and O2. Recorded data from the EEG cap was amplified with a g®.USBamp amplifier and then transferred via USB to a secured laptop running BCI2000. The BCI2000 software allows for running the algorithm (i.e., presenting the visual stimuli) and for storing EEG data. To minimize environmental noise, data collection took place in a dimmed quiet room with white noise in the background. Since data collection was performed at an external facility, the testing setting could not be heavily controlled, and the testing setting was not consistent as the facilities differed at each location. The study was approved by East Carolina University's Medical Center Institutional Review Board, Appendix B.

The visual presentation composed of six categories which include familiar face, upside-down familiar face, unfamiliar face, upside-down unfamiliar face, random objects, and upside-down

random objects. Each stimulus type is presented to the research subject 20 times, referred to as 20 epochs or trials. Familiar faces included the faces of 4 presidents: Trump, Obama, Nixon and Lincoln. These faces were shown to each participant before testing to ensure familiarity. Unfamiliar faces were generic faces found on Google (4 male and 4 female) while random objects involved 4 flowers.

4.2 Pre-processing

Raw data was preprocessed utilizing MATLAB with a built-in EEGLAB toolbox to remove the unwanted artifacts. A bandpass filter was used to remove some of these artifacts with cut-off frequencies of 1 Hz and 30 Hz. Newly cleaned data are then epoched into 1500ms increments (500ms before stimulus and 1000ms after stimulus) and averaged, referred to as the subject's averaged ERP, for each stimulus category (n=6). Therefore, each participant has 6 pieces of data for each stimulus category. However, in this thesis, the focus will be on the familiar face stimuli data. The familiar face stimuli category is used to analyze MCI subjects and their ability to retrieve memory to recognize the president's faces. The expectation is that MCI subjects would process familiar faces worse than healthy subjects and it should be represented in the results.

4.3 Time-domain analysis

Time-domain analysis was performed and analyzed briefly. Each subject's averaged ERP was visually inspected for signal quality and for overall cleanliness of the signal. Any subject with undesirable waveforms due to signal quality was excluded from the study. The subjects were then organized into groups, MCI and normal controls (NC), based on their respective MoCA scores.

MCI is categorized as a MoCA score equal to or under 26 and normal controls as a MoCA score above 26.

After eliminating subjects with noisy data and organizing the subjects into their respective groups, the resulting number of subjects is 18 total with 10 subjects in the NC group and 8 subjects in the MCI group. The NC group has a MoCA score of 28.7 ± 1.4 and the MCI group has a MoCA score of 18.1 ± 4.3.

4.4 Functional Connectivity Analysis

To calculate wPLI, a toolbox created by East Carolina University's Sensory-Motor Integration Lab (SMILe) was adopted. This toolbox involves the use of the Morlet wavelet transform to gather time-frequency domain data. The Morlet wavelet transform convolves a complex Morlet wavelet kernel (Gaussian-windowed sine wave) with the pure time series signal [46]. Morlet kernels are composed for each frequency ranging from 4 – 30Hz. The Morlet wavelet transform is performed with each EEG channel signal. Therefore, the convolution of the EEG signal with the Morlet kernel is performed for each kernel/frequency between 4-30 Hz. This creates a matrix of channel x frequency x time x trials.

The use of the Morlet wavelet transform results in a complex signal that allows for phase information to be extracted at each time point at a specific frequency [46]. There is a major benefit in using the Morlet wavelet transform since it allows for time and frequency information to be extracted simultaneously. Processing would not strictly be in time or frequency domain but rather allow for gathering of time-frequency data. Fig. 14 illustrates the convolution of a Morlet wavelet

kernel (1 Hz) and an EEG signal to extract complex data that allows for further extraction of instantaneous phase.

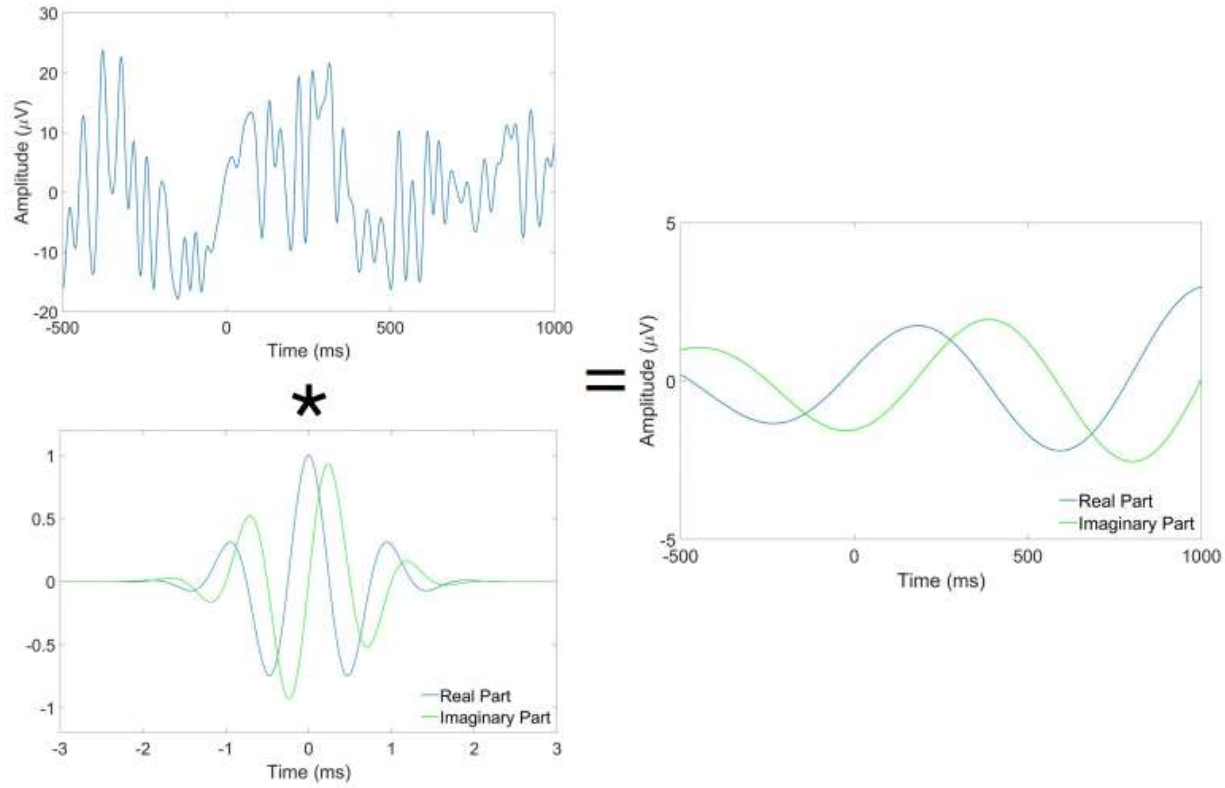

Figure 14: Expansion of the Morlet wavelet transform. EEG channel signal convolved with a 1Hz Morlet kernel resulting in the Morlet wavelet transform equivalent of the EEG channel signal.

The time-frequency cross-spectrum was calculated for each channel combination by multiplying one channel by the conjugate of the second channel, refer to Fig. 15. With 16 channels, there are 120 channel combinations. Utilization of the time-frequency cross-spectrum allows for extraction of phase differences between the two channels analyzed. Since the Morlet wavelet transform was used to collect time-frequency data, the instantaneous phase differences can be extracted at each time point and at each frequency point. The time-frequency cross-spectrum data was consolidated in a 5D matrix of channel by channel by frequency by time by trials.

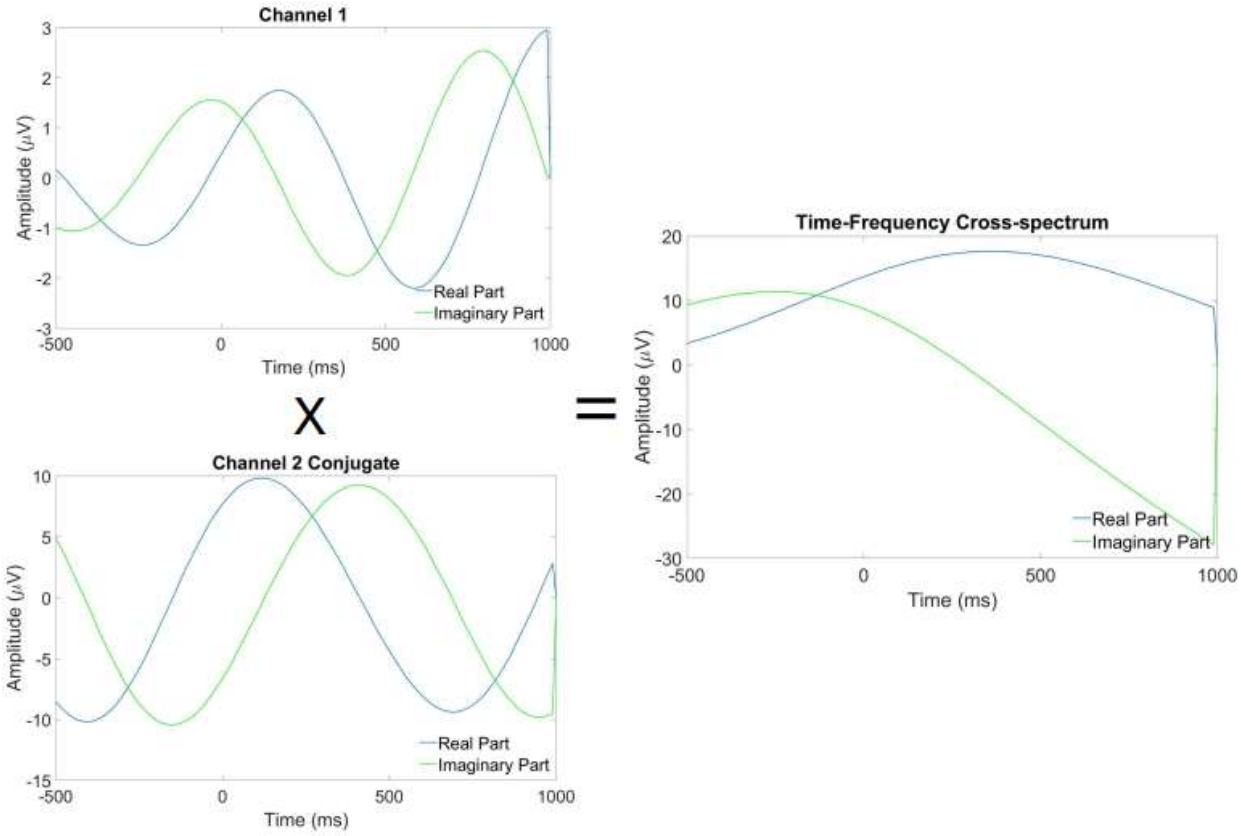

Figure 15: Expansion of the time-frequency cross-spectrum calculation. Multiplication of the channel 1 signal by the complex conjugate of the channel 2 signal results in the respective time-frequency cross-spectrum.

The data was divided into the different frequency bands and averaged along the frequency bands to output 4D data of channel x channel x time x trials. The frequency bands were defined as follows: theta (4-8Hz), alpha (8-13Hz), mu/upper alpha (10-12Hz) and beta (13-30Hz). For each frequency band, there will be individual 4D data.

wPLI was be calculated at each frequency band. Monte Carlo simulations were performed based on 15 randomly picked trials out of the original 20 trials (15 permutations), repeated 1000 times. This Monte Carlo simulation creates a probability distribution given the original sample. By

running multiple simulations, a statistical distribution is formed where the most probable outcome is emphasized while also adding variability. The use of the Monte Carlo simulation creates an unbiased representative group based on the original samples, therefore, the 20 trials expand to 1000 simulations. With a larger sample size, the average comes closer to the expected value. The 1000 simulations have a higher statistical strength compared to the 20 original trials. These simulations are used to calculate wPLI based on the imaginary component of the cross-spectrum (imagcs), Equation 6. To eliminate possible volume conduction biases, wPLI values of 1 are eliminated, thus wPLI values indicating phase differences 0 mod π.

$$\text{wPLI} = \frac{\left|E\{\Im\{X\}\}\right|}{E\{|\Im\{X\}|\}} \tag{6}$$

Fig. 16 illustrates a small sample of Monte Carlo simulations and the resulting averaged wPLI value (black line). To reiterate, the wPLI is averaged among all 1000 simulations per subject in each frequency band.

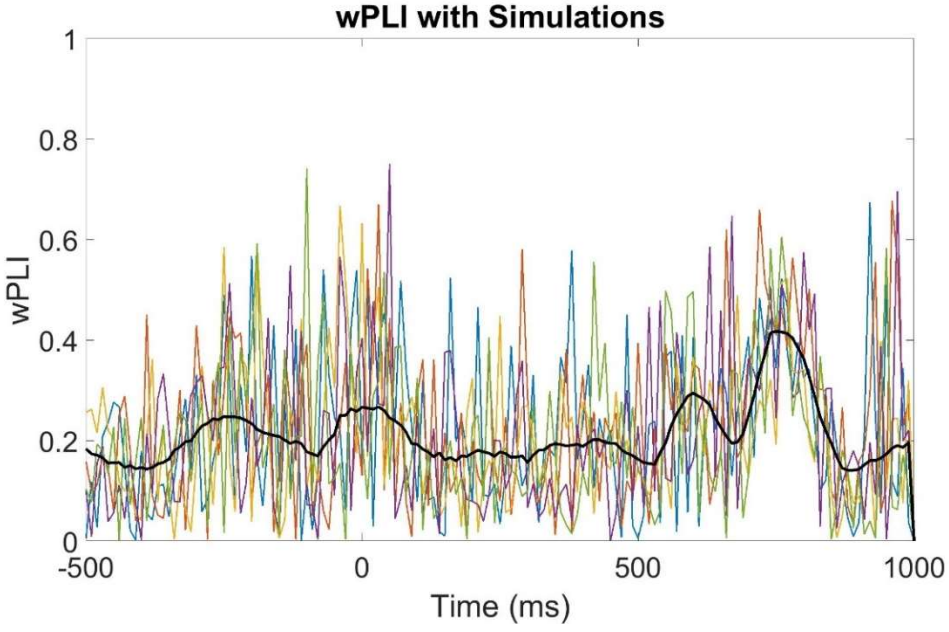

Figure 16: Monte Carlo simulations of wPLI calculations with the averaged wPLI values over time.

It required numerous steps to gather wPLI data from raw EEG data. This starts with the Morlet Wavelet transform to calculation of the time-frequency cross-spectrum and finally calculating the wPLI through Monte Carlo simulations. Table 3 summarizes the steps and alterations in data structure after each step.

Table 3: Steps to calculate and consolidate wPLI data.

Steps	Data Structure
Morlet Wavelet cross-spectrum	Channel x channel x frequency x time x trials
Split into frequency bands	Channel x channel x time x trials (for each band)
Monte Carlo and wPLI calculation	Channel x channel x time x simulations (for each band)
Average among simulations	Channel x channel x time (for each band)

4.4.1 Channel combination groupings

Given numerous channel pairs, they are divided into different groups. These groups include the inter-hemispheric, intra-hemispheric, and transverse [48, 49]. Fig. 17 illustrates these channel groupings. Inter-hemispheric interactions are channel pairs that connect the left and right hemispheres, along the coronal plane Fig. 17 (a) [48, 49]. Intra-hemispheric interactions are channel pairs along the longitudinal plane within the same hemispheres, Fig. 17 (b,d) [48, 49]. Transverse interactions are also localized based on interactions within the same hemispheres; however, it involves all the channel pairs aside from just longitudinal interactions, Fig. 17 (c) [47]. Intra and inter hemispheric can further be divided into short and long based on channel distances, i.e. intra-hemispheric short are channel pairs that are close to each other (Fig. 17 d) and intra-hemispheric long are channel pairs that are far from each other (Fig. 17 b) [28, 48]. Referring to Fig. 17 (a), inter-hemispheric short would refer to channel pairs similar to Fp1-Fp2, F3-F4, C3-C4, etc. while inter-hemispheric long are the channel pairs similar to F7-F8, T3-T4, and T5-T6

[47]. These groupings ignore any channel interactions involving the electrodes placed along the midline.

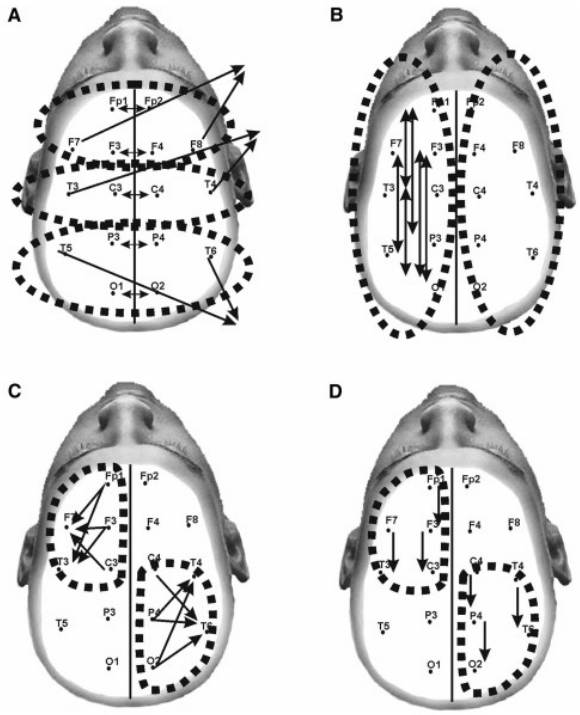

Figure 17: Example of channel groupings set forth by the Neuroscience field which include (a) inter-hemispheric, (b) intra-hemispheric long, (c) transverse, and (d) intra-hemispheric short interactions [47].

For this thesis, the 120 channel pairs are grouped into intra-hemispheric short, intra-hemispheric long, inter-hemispheric short, inter-hemispheric long, and transverse channel groups. Intra-hemispheric short (intrashort) interactions were defined interactions along the longitudinal plane that are one electrode apart, such as F3 and C3. Intra-hemispheric long (intralong) defined as two electrodes apart such as F3 and P3. Inter-hemispheric interactions were interactions along the coronal plane that crossed hemispheres where short is defined as two channels apart (intershort)

and long as three channels apart (interlong). Transverse interactions (transverse) are within the same hemispheres, defined as one electrode apart with any interaction that is not in the longitudinal direction.

After sorting all the channel pairs into their respective categories, only 32 out of the 120 channel pairs fit a category, Fig. 18. Most of the channel pairs that did not fit a category involved interactions with mid-line electrodes while some pairs had long distances such as F7 and O1 (too long to be categorized as intra-hemispheric long interactions). Other channel pairs that were not grouped included inter-hemispheric transverse interactions such as F7 and P4, the inter-hemispheric group is defined as strictly coronal interactions while the transverse group is localized as within the same hemisphere. Fig 16 illustrates all the channel pairs in each category. The wPLI data was averaged within each channel group. Therefore, the average of the channel pairs of F3-C3, C3-P3, P3-O1, F4-C4, C4-P4, and P4-O2 will make up the averaged wPLI for the intra-hemispheric short category.

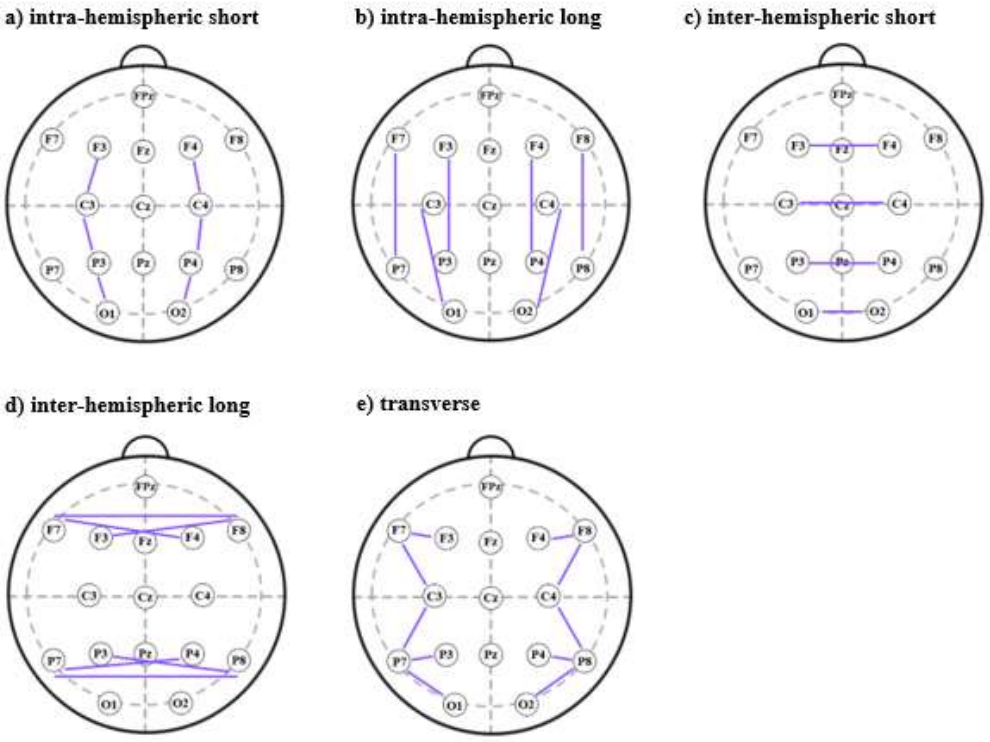

Figure 18: Thesis channel pairs sorted into 5 groups based on 120 channel combinations from 16 electrodes.

Dividing channel pairs into multiple groups allows for evaluation of different types of interactions. Previous research involved averaging amongst all channel pairs. However, averaging among all pairs does not allow for in-depth analysis of different types of neural interactions. With the channel combination groups, intra-hemispheric interactions and inter-hemispheric interactions can be analyzed separately. Specific types of interactions can be analyzed separately rather than as a whole.

4.6 Statistical Analysis

To analyze the difference between NC and MCI, the wPLI difference value is analyzed. The wPLI difference, $\Delta wPLI_{P300,}$ is calculated as the difference between wPLI in the P300 and baseline time frame per each subject. These values were calculated based on the average wPLI value around 200-360ms, $wPLI_{P300}$, subtracted by the average wPLI value around 0ms to 100ms, $wPLI_{base}$. This calculation can be seen in Equation 7. Since individual subjects may not have the same baseline wPLI value, the difference between P300 and baseline is used to better represent the fluctuation due to the visual stimuli of familiar face.

$$\Delta \mathrm{wPLI}_{\mathrm{P300}} = \overline{\mathrm{wPLI}_{\mathrm{P300}}} - \overline{\mathrm{wPLI}_{\mathrm{base}}} \quad (7)$$

One way ANOVA was used to test differences between MCI and healthy controls. Since there are differences in sample sizes, MCI (n=8) and NC (n=10), a student's t-test cannot be performed. With 4 frequency bands and 5 channel combination groups, a total of 20 individual ANOVA tests were performed to test each condition. ANOVA was performed within MATLAB to gather p-values where a p-value < 0.05 was considered significant.

Chapter 5. Results

With time domain analysis, it allows for evaluation of EEG activity over time. Fig. 19 illustrates grand-averaged ERPs at channels Cz and Pz. These two channels are popular electrodes that are used to evaluate cognitive functions. However, at these two channels, the P300 ERP (250-300ms) illustrates no difference between MCI and healthy controls. Towards the 900ms-1000ms time frame, there does seem to be some separation where MCI have a slightly higher amplitude than healthy controls. Since this separation is 900ms post-stimulus, it may be too long past the stimulus to provide any significant information regarding familiar face processing.

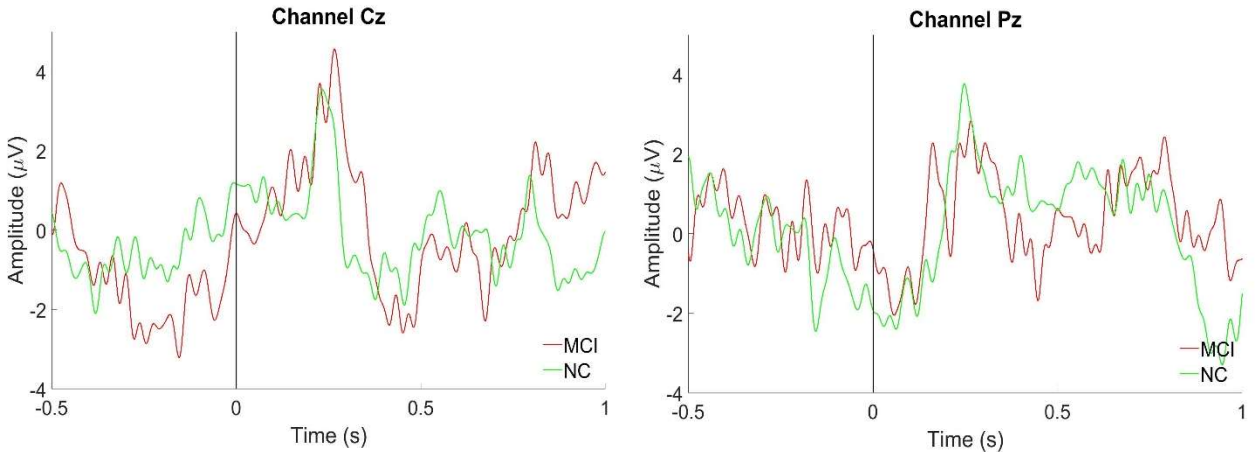

Figure 19: MCI and NC grand averaged ERPs for channels Cz and Pz.

Fig. 20 displays the wPLI functional connectivity between the channels Cz and Pz. This figure is used to illustrate the difference in information between time-domain EEG (Fig.19) and time-frequency domain functional connectivity (Fig. 20). With time-domain EEG, analysis can only be performed based on individual channels. Functional connectivity allows for analysis of interactions between channels. Fig. 19 illustrates traditional EEG time domain analysis while Fig. 20 illustrates the use of functional connectivity allowing for analysis of the neuron interactions between Cz and Pz local brain regions.

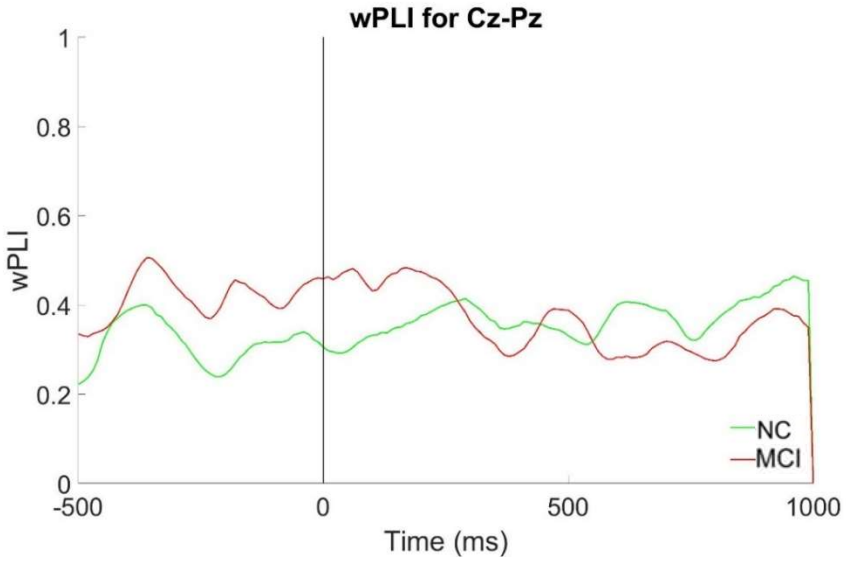

Figure 20: Functional connectivity, wPLI, of the channel pair Cz-Pz.

To reiterate, functional connectivity (wPLI) was analyzed per frequency band and per channel combination groups. The first channel combination group is the intrashort channel group, composed of channel pairs within the same hemisphere that are separated by a short distance. Fig. 21 illustrates the grand-averaged wPLI at the Mu frequency band in the intrashort channel group with error bars. wPLI in -500ms to -250ms for both MCI and healthy controls are relatively equal indicating a good baseline time interval. Starting at -250ms, MCI subjects illustrates a slow increase in wPLI over time until roughly 200ms then decreasing back to roughly baseline. However, healthy controls do not show as much of an increase in wPLI leading to some separation in wPLI from 0ms to 200ms. In Fig. 21, MCI seem to have a wPLI maximum at around 150ms and healthy controls seem to have a wPLI maximum at around 300ms.

Figure 21: Intra-hemispheric short channel group wPLI over time in the Mu frequency band

The second channel combination group, intralong channel group, is illustrated in Fig. 22 with the mu frequency band. In this channel group and frequency band, the -500ms to -250ms time interval also illustrates a good time frame as baseline since MCI and healthy controls are relatively equal. There is still some separation in wPLI around 0ms to 200ms. In this channel group, it also shows MCI to have a gradual increase in wPLI occurring earlier than healthy controls.

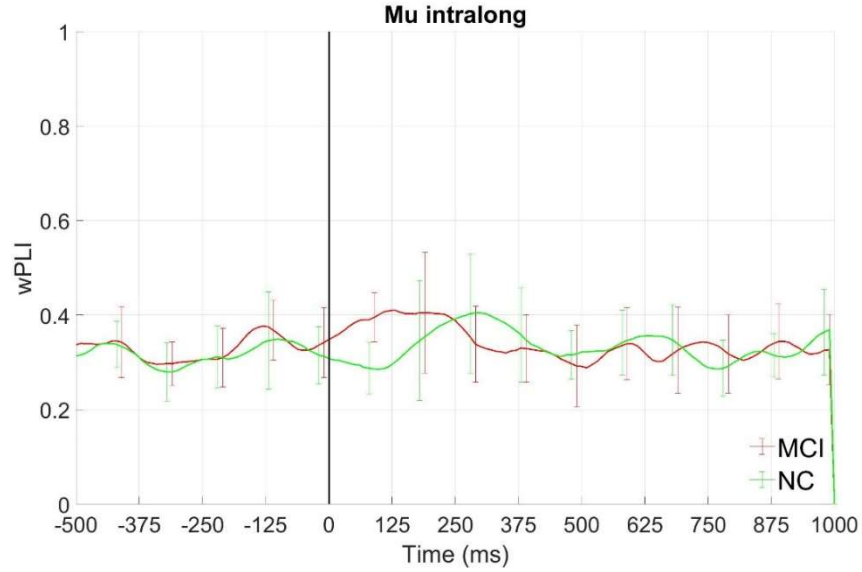

Figure 22: Intra-hemispheric long channel group wPLI over time in the Mu frequency band.

Fig. 23 illustrates the intershort channel group in the alpha frequency band for grand-averaged wPLI. Pre-stimulus does not show as good as a baseline as the mu frequency band in the intra-short and intra-long channel groups (Fig. 21 & Fig. 22). For baseline, there is a slight separation between MCI and healthy controls with overlapping error bars. Healthy controls illustrate an increase in wPLI where the maximum peak is observed at around 250ms. This trend is not observed in MCI subjects. MCI subjects have a slightly elevated baseline that remained fairly constant over the full 1500ms.

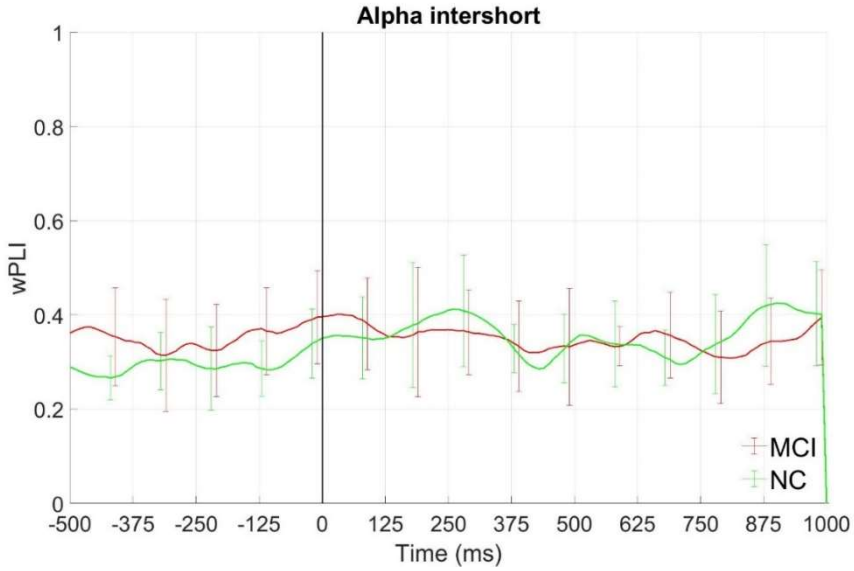

Figure 23: Inter-hemispheric short channel group wPLI over time in the Alpha frequency band

The theta frequency band is used to illustrate the interlong channel group in Fig. 24. MCI shows a higher wPLI during all of post-stimulus from 0ms to 1000ms where the largest separation is best observed around 100ms to 200ms. MCI have an increase in wPLI post-stimulus with a peak around 150ms while healthy controls do not show an increase in wPLI at all.

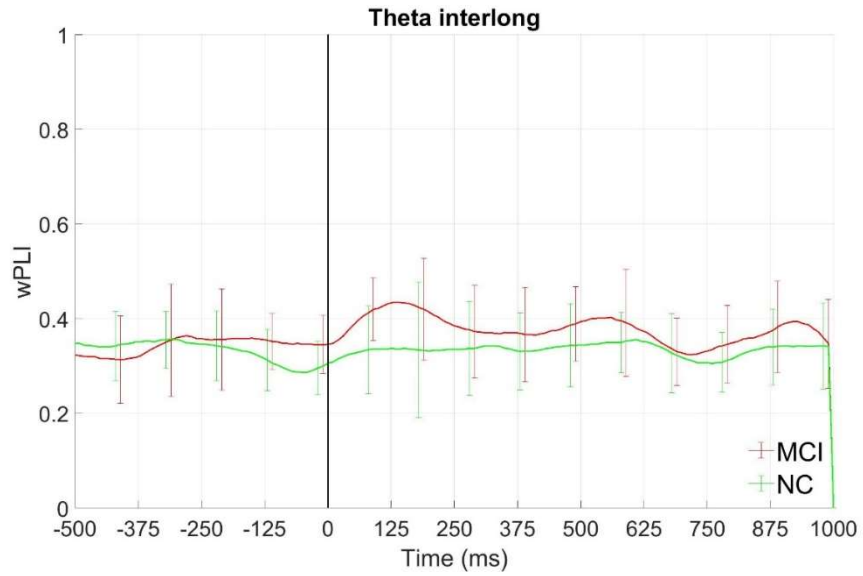

Figure 24: Inter-hemispheric long channel group wPLI over time in the Theta frequency band.

The last channel group is the transverse channel group. Fig. 25 illustrates the beta frequency band grand-averaged wPLI in the transverse channel group. Healthy controls had the same relative wPLI over all pre-stimulus and all post-stimulus, -500ms to 1000ms. MCI is observed to have a slight increase in wPLI starting at around -200ms until 0ms then remaining fairly constant.

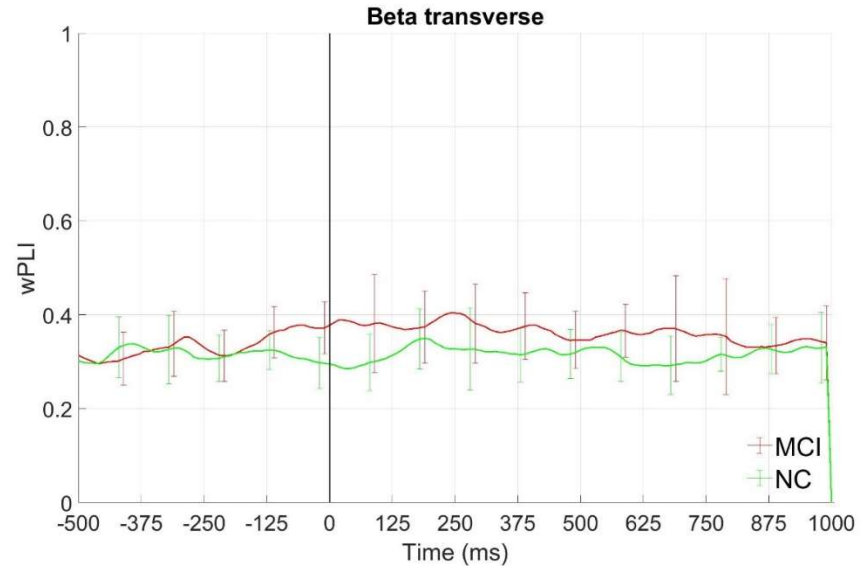

Figure 25: Transverse channel group wPLI over time in the Beta frequency band

In the theta, mu and alpha frequency band channel combination groups, MCI and NC have consistent wPLI trends among the frequency bands. In these frequency bands, it is observed that subjects with MCI tend to have a higher baseline with a higher wPLI at the time of stimulus presentation (~0 ms) compared to NC. MCI start at a higher baseline wPLI then are observed to have an increase in FC starting at ~0ms and continuing to increase through ~100-200ms. This increase in FC should not be due to the visual stimuli as this latency occurs too early for it to be a representation of any cognitive process in response to stimuli. However, the early increase in FC could be a representation of MCI subjects predicting the visual stimuli presentation. MCI start experiencing an increase in wPLI right at stimulus presentation, this is too fast of a response. NC have a more expected response where the increase in wPLI occurs around the P300 time frame, starting around ~200 ms. These responses from MCI and NC are consistent through theta, alpha, and mu frequency band channel combination groups.

In the beta band channel combination groups, MCI also have a higher baseline compared to NC. The higher baseline is only slightly higher among MCI subjects. There is no obvious increase in FC post stimulus from MCI or NC subjects observed in the beta frequency band.

For statistical analysis, the difference value between the P300 and baseline, $\Delta wPLI_{P300}$, was used. Since MCI consistently had a higher starting baseline (~0ms) compared to NC throughout all frequency band and channel combination group conditions, use of $\Delta wPLI_{P300}$ offers a better representation of the visual stimuli response compared to just the wPLI values centered around P300. The $\Delta wPLI_{P300}$ values offer a representation of fluctuation in wPLI due to the familiar face stimuli. Fig. 26 illustrates the $\Delta wPLI_{P300}$ values in the mu band. NC have a higher $\Delta wPLI_{P300}$ in

most of the channel combination groups specifically in the intrashort, intralong, and intershort channel groups. In the interlong channel group, the mean value is only slightly higher in the NC group. The mean $\Delta wPLI_{P300}$ in the transverse group is essentially equal between the two subject groups.

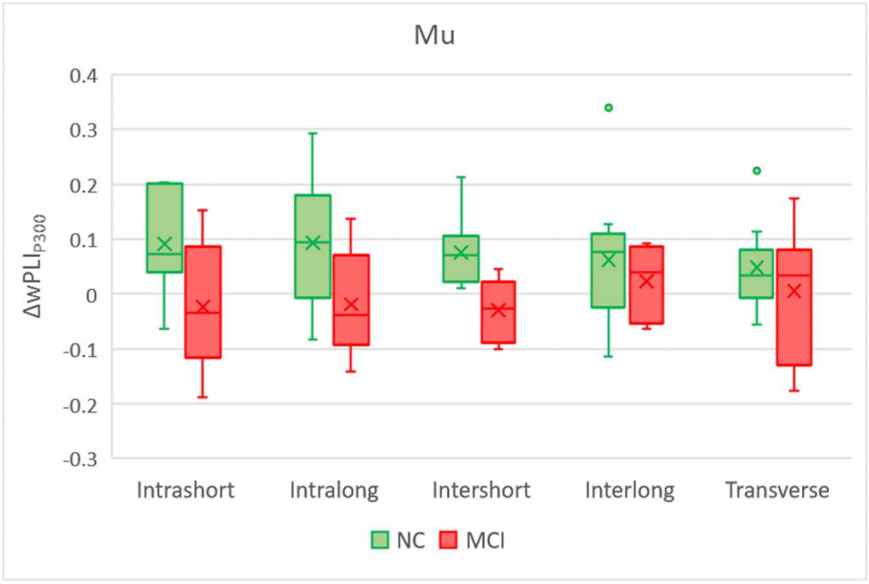

Figure 26: Mu band $\Delta wPLI_{P300}$ values in all 5 channel combinations groups of intra-hemispheric short (intrashort), intra-hemispheric long (intralong), Inter-hemispheric short (intershort), inter-hemispheric long (interlong), transverse.

The $\Delta wPLI_{P300}$ values for the alpha band can be seen in Fig. 27. NC also has an overall higher $\Delta wPLI_{P300}$ than MCI, however, it is not as distinct as the Mu band. Even though the mu band is within the alpha band, the $\Delta wPLI_{P300}$ differences between MCI and NC are not as well observed. Again, the interlong and transverse channel groups show very little difference between the subject groups.

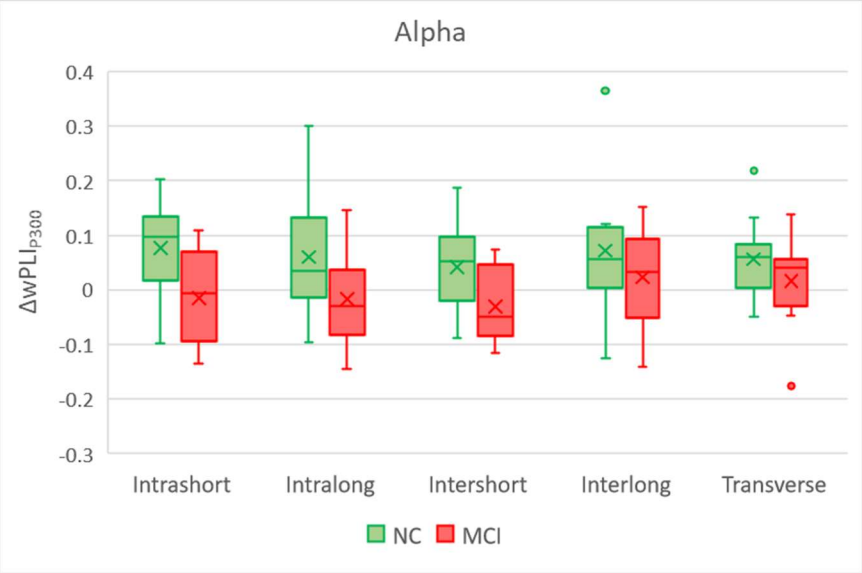

Figure 27: Alpha band $\Delta wPLI_{P300}$ values in all 5 channel combinations groups of intra-hemispheric short (intrashort), intra-hemispheric long (intralong), Inter-hemispheric short (intershort), inter-hemispheric long (interlong), transverse.

The one-way ANOVA results for all frequency bands are contained in Table 4, comparing $\Delta wPLI_{P300}$ between MCI and NC. Since there are 4 frequency bands with 5 channel combination groups, a total of 20 individual one-way ANOVA tests were performed. Out of these 20 tests, there were 4 tests that yielded statistically significant p-values. These 4 tests are the alpha intra-hemispheric short (p-value = 0.0423), mu intra-hemispheric short (p-value = 0.0286), mu intra-hemispheric long (p-value = 0.0477), and the mu inter-hemispheric short (p=0.0423).

Table 4: One-way ANOVA results testing $\Delta wPLI_{P300}$ differences between MCI and NC subjects.

Frequency Band	Channel Combo	p-val
Theta 4-8 Hz	Intrashort	0.5052
	Intralong	0.9561
	Intershort	0.643
	Interlong	0.7089
	transverse	0.5242
Alpha 8-13 Hz	Intrashort	0.0423 *
	Intralong	0.1407
	Intershort	0.0619
	Interlong	0.3843
	transverse	0.3457
Mu/Upper Alpha 10-12 Hz	Intrashort	0.0286 *
	Intralong	0.0477 *
	Intershort	0.0018 **
	Interlong	0.4353
	transverse	0.3806
Beta 13-30 Hz	Intrashort	0.5673
	Intralong	0.4964
	Intershort	0.0898
	Interlong	0.4446
	transverse	0.3057

Chapter 6. Discussion

The use of functional connectivity analysis opens another way to analyze EEG data compared to traditional time domain analysis. Time domain analysis involved analyzing EEG and ERPs by looking at amplitudes and latencies, at specific electrodes. Each electrode would be analyzed separately. The application of functional connectivity analysis grants holistic information to be extracted. Channel pairs are analyzed to examine the underlying neuronal networks and interactions between two brain regions.

Functional connectivity via PLI and wPLI has previously indicated a difference between AD/MCI and healthy controls using resting state EEG data. This study indicates that the same decrease in wPLI can also be observed with ERP data, providing a possible diagnostic tool to detect early onset of Alzheimer's disease. Further longitudinal testing with this subject group is needed. Since resting state EEG data was not collected, it cannot be determined if the difference in wPLI is more prominent in resting state EEG or visually evoked ERP data. The use of the wPLI method for analyzing FC eliminates all possible volume conduction biases, where neighboring channels pick up the same source signal causing false synchronization. Volume conduction bias is eliminated by removing any phase differences around 0 mod π. Therefore, the results strongly indicate MCI have a lower functional connectivity in the mu and alpha frequency bands. To reiterate, the wPLI method also eliminates strong FC between channels, brain regions. By eliminating some of the strong synchronization, there were still statistically significant results indicating $\Delta wPLI_{P300}$ differences between MCI and NC.

All 4 conditions that were statistically significant were in the frequency range of 8-13 Hz. Mu is a special subset of the alpha band where the mu frequency range can be considered as upper alpha. The alpha band is considered to be associated with memory processes which correlate with the study's use of familiar face stimuli. Dementia is defined as having memory deficits with tasks, objects, and with people. In severe dementia patients, they often have difficulty recognizing familiar people such as family. Therefore, MCI subjects are expected to have a harder time processing familiar faces and it is not surprising that FC was observed to be decreased in the alpha frequency band. The mu band is associated with sensorimotor which does not correspond with visual stimuli. However, the mu frequency range is within the alpha frequency range. Therefore, the results could be more associated with alpha band's memory processing rather than mu's sensorimotor. The decrease in synchronization observed among MCI subjects is most likely due to memory deficits with regards to processing these visual stimuli as a familiar face.

MCI's decrease in synchronization could be linked to the physiological effects of dementia where neurons become weakened due to the Aβ and NFTs. The weakened neurons should have a slower conduction and therefore could affect the synchronization with neighboring neurons. MCI patients may also have lower activation of the neurons.

Within the frequency bands, the channel combinations groups with statistical significance are the intra-hemispheric short, intra-hemispheric long, and inter-hemispheric short channel interactions. There are two pathways for visual processing, dorsal and ventral [48, 49]. The dorsal visual pathway travels from the occipital lobe to parietal lobe to frontal lobe, from the back to the front of the brain [49]. The ventral visual pathway travels from the occipital lobe to the temporal lobe

[49]. The dorsal and ventral visual pathways are associated with answering “where” and “what” respectively [48, 49]. However, it is not exclusive in which both “where” and “what” processing are observed in each pathway [48]. The intra-hemispheric channel combination groups correlate with the dorsal visual processing pathway, FC does not analyze directionality but the channel pairs in the intra-hemispheric group involve interactions occurring longitudinally. These channel pairs are located along the dorsal visual pathway. Since the intra-hemispheric group includes channel pairs that associate with the dorsal visual pathway, the results further reflect MCI’s deficit in familiar face processing. Statistical significance observed in intra-hemispheric channel groups, reflects a deficit in MCI subjects processing the visual stimuli, most likely from processing familiar faces due to memory deficits.

The mu frequency band inter-hemispheric short interaction resulted in a very strong statistical significance ($p < 0.01$). These include channel pairs across hemispheres. A strong difference between MCI and NC could indicate an imbalance of hemispheres. NC may have uniform processing through both left and right hemispheres, where both hemispheres are equally active. MCI could experience a lack of balance where one hemisphere is less active than the other.

This research study could be greatly improved. There was a total of 18 subjects that were used in data analysis, this sample size should be increased. These subjects were also recorded at numerous facilities, different senior centers. Keeping the EEG recording location consistent among all subjects will allow for a more controlled environment. Many of these senior centers were not optimal for EEG recording, noise and light could not be best controlled at these locations. The recording location should be dark and quiet for optimal recording.

Data was also collected using a 16-channel headset, use of more channels such as 32 or 64 channels will allow for a more in-depth analysis of various types of channel interactions. In the channel combinations groups in this study, there were few channel pairs that were included in each group. Using a headset with more channels will include more channel pairs in each channel combination group, increasing the number of interactions that can be evaluated. Even more channel combination groups can be created, this study only sorted the channel pairs by hemispheric interactions. However, channel pairs could also be sorted based on brain lobes such as occipital and parietal lobes. The channel combination groups in this study can also only be used to reflect the dorsal visual pathway. With the 16-channel headset, there were no electrodes placed on the temporal lobe lacking channel pairs that would reflect the ventral visual pathway.

This study only observed differences in the strength of functional connectivity between MCI and NC subjects. Further analysis, via graph theory, would allow for a better analysis of connectivity patterns. The protein aggregates, weakened neurons, may cause MCI subjects to develop an alternative connectivity pathway to accomplish the same cognitive task. Graph theory will allow for an examination of connectivity pattern differences between MCI and NC subjects.

Chapter 7. Conclusion

Functional connectivity can be an extremely useful analysis method to distinguish the development of dementia from normal aging. FC should also be implemented as a standard of care for MCI patients to monitor progression of dementia. When using a familiar face visual stimulus, MCI subjects showed a lower change in wPLI, $\Delta wPLI_{P300,}$ in response to the stimuli compared to NC subjects in the mu and alpha frequency bands. The mu frequency range is within the alpha frequency range, therefore, the differences in $\Delta wPLI_{P300}$ could be a reflection of the impact of dementia on memory processing. wPLI provides insight to subtle network-level changes of the brain which manifest themselves as synchronization differences where MCI with a lower $\Delta wPLI_{P300}$ indicates lower synchronization by MCI subjects in response to stimuli, most possibly related to diminished memory processing.

References

[1] "Alzheimer's and Dementia." alz.org. https://www.alz.org/alzheimers-dementia/facts-figures. (accessed July 20, 2021)

[2] S. Hoops, S. Nazem, A. Siderowf, J. Duda, S. Xie, M. Stern, and D. Weintraub, "Validity of the MoCA and MMSE in the detection of MCI and dementia in Parkinson disease," Neurology, vol. 73, no. 21, pp. 1738-1745, Nov. 2009, doi: 10.1212/WNL.0b013e3181c34b47

[3] S. McLenna, J. Mathias, L. Brennan, and S. Stewart, "Validity of the Montreal Cognitive Assessment (MoCA) as a Screening Test for Mild Cognitive Impairment (MCI) in a Cardiovascular Population," Journal of Geriatric Psychiatry and Neurology, vol. 24, no. 1, pp. 33-38, Dec. 2010, doi: 10.1177/0891988710390813

[4] L. Mosconi, A. Pupi, and M. De Leon, "Brain glucose hypometabolism and oxidative stress in preclinical Alzheimer's disease," Annals of the New York Academy of Sciences, vol. 1147, pp. 180-195, Dec. 2008, doi: 10.1196/annals.1427.007

[5] "M. Tabert, et. al., ""Neuropsychological Prediction of Conversion to Alzheimer Disease in Patients With Mild Cognitive Impairment,"" Archives of General Psychiatry, vol. 63, pp. 916-924, Aug. 2006, doi:10.1001/archpsyc.63.8.916"

[6] "Alzheimer's and Dementia: 10 signs." alz.org. https://www.alz.org/alzheimers-dementia/10_signs. (accessed July 20, 2021)

[7] S. Sadigh-Eteghad et al., “Amyloid-Beta: a crucial factor in Alzheimer’s Disease,” Medical Principles and Practice, vol. 24, pp. 1-10, 2015, doi: 10.1159/000369101

[8] M. Murphy, and H. LeVine, “Alzheimer’s disease and the amyloid-beta peptide,” Journal of Alzheimer’s Disease, vol. 19, no. 1, pp. 311-323, 2010, doi: 10.3233/JAD-2010-1221

[9] A. Metaxas, and S. Kempf, “Neurofibrillary tangles in Alzheimer’s disease: elucidation of the molecular mechanism by immunohistochemistry and tau protein phosphor-proteomics,” Neural Regeneration Research, vol. 11, no. 10, pp. 1579-1581, Oct. 2016, doi: 10.4103/1673-5374.193234

[10] S. Camandola and M. Mattson, "Brain metabolism in health, aging, and neurodegeneration," EMBO Journal, vol. 36, no. 11, pp. 1474-1492, Jun. 2017, doi: 10.15252/embj.201695810

[11] K. Do et al., "The effects of exercise on hypothalamic neurodegeneration of Alzheimer's disease mouse model," PLoS One, vol. 13, no. 1, Jan. 2018, doi: 10.1371/journal.pone.0190205

[12] A. Jackson, and D. Bolger, "The neurophysiological bases of EEG and EEG measurement: a review for the rest of us," Psychophysiology, vol. 51, no. 11, pp. 1061-1071, Nov. 2014, doi: 10.1111/psyp.12283

[13] "International 10-20 system for EEG-MCN." wikimedia.org. https://commons.wikimedia.org/wiki/File:International_10-20_system_for_EEG-MCN.svg (accessed July 15 2021)

[14] C. Papadaniil, V. Kosmidou, A. Tsolaki, M. Tsolaki, I. Kompatsiaris, and L. Hadjileontiadis, "Cognitive MMN and P300 in mild cognitive impairment and Alzheimer's disease: A high density EEG-3D vector field tomography approach," Brain Research, vol. 1648, pp. 425-433, Jul. 2016, doi: 10.1016/j.brainres.2016.07.043

[15] R. Newsome, C. Pun, V. Smith, S. Ferber, and M. Barense, "Nueral correlates of cognitive decline in older adults at-risk for developing MCI: Evidence from the CDA and P300," Cognitive Neuroscience, vol. 4, no. 3-4, pp.152-162, Nov. 2013, doi: 10.1080/17588928.2013.853658

[16] S. Jiang, C. Qu, F. Wang, Y. Liu, Z. Qiao, X. Qui, X. Yang, and Y. Yang, "Using event-related potential P300 as an electrophysiological marker for differential diagnosis and to predict the progression of mild cognitive impairment: a meta-analysis," Neurological Sciences, vol. 36, no. 7, pp. 1005-1112, Jul. 2015, doi:10.1007/s10072-015-2099-z

[17] J. van Deursen, E. Vuurman, L. Smits, F. Verhey, and W. Riedel, "Response speed, contingent negative variation and P300 in Alzheimer's disease and MCI," Brain and Cognition, vol. 69, no. 3, pp. 592-599, Apr. 2009, doi: 10.1016/j.bandc.2008.12.007

[18] M. Nentwich, L. Ai, J. Madsen, Q. Telesford, S. Haufe, M. Milham, and L. Parra, "Functional connectivity of EEG is subject-specific, associated with phenotype, and different from fMRI," NeuroImage, vol. 218, May 2020, doi: 10.1016/j.neuroimage.2020.117001

[19] V. Sakkalis, "Review of advanced techniques for the estimation of brain connectivity measured with EEG/MEG," Computers in Biology and Medicine, vol. 41, no. 12, pp. 1110-1117, Dec. 2011, doi: 10.1016/j.compbiomed.2011.06.020

[20] A. Bastos, and J. Schoffelen, "A tutorial review of functional connectivity analysis methods and their interpretational pitfalls," Frontiers in Systems Neuroscience, vol. 9, no. 175, Nov. 2016, doi: 10.3389/fnsys.2015.00175

[21] H. Wang, C. Benar, P. Quilichini, K. Friston, V. Jirsa, and C. Bernard, "A systematic framework for functional connectivity measures," Frontiers in Neuroscience, vol. 8, no. 405, Dec. 2014, doi: 10.3389/fnins.2014.00405

[22] M. Guevara, and M. Corsi-Cabrera, "EEG coherence or EEG correlation?," International Journal of Psychophysiology, vol. 23, no. 3, pp. 145-153, Oct. 1996, doi: 10.1016/S0167-8760(96)00038-4

[23] M. Brazier, and J. Casby, "An application of the M.I.T. digital electronic correlator to a problem in EEG: the EEG during mental calculation," Electroencephalography and Clinical Neurophysiology, vol. 3, no. 375, 1951.

[24] "Cross-correlation." wikipedia.org. https://en.wikipedia.org/wiki/Cross-correlation (accessed July 7, 2021)

[25] S. Bowyer, "Coherence a measure of the brain networks: past and present," Neuropsychiatric Electrophysiology, vol. 2, no. 1, Jan. 2016, doi: 10.1186/s40810-015-0015-7

[26] C. Besthorn, H. Forstl, C. Geiger-Kabisch, H. Sattel, T. Gasser, and U. Schreiter-Gasser, "EEG coherence in Alzheimer disease," Electroencephalography and clinical Neurophysiology, vol. 90, no. 3, pp. 242-245, Mar. 1994, doi: 10.1016/0013-4694(94)90095-7

[27] R. Srinivasan, W. Winter, J. Ding, and P. Nunez, "EEG and MEG coherence: Measures of functional connectivity at distinct spatial scales of neocortical dynamics," Journal of Neuroscience Methods, vol. 166, no. 1, pp. 41-52, Oct. 2007, doi: 10.1016/j.jneumeth.2007.06.026

[28] C. Stam, G. Nolte, and A. Daffertshofer, "Phase lag index: assessment of functional connectivity from multi channel EEG and MEG with diminished bias from common sources," Human Brain Mapping, vol. 28, no. 11, pp. 1178-1193, Nov. 2007, doi: 10.1002/hbm.20346

[29] P. Nunez, R. Srinivasan, A. Westdorp, R. Wijesinghe, D. Tucker, R. Silberstein, and P. Cadusch, "EEG coherency I: statistics, reference electrode, volume conduction, Laplacians, cortical imaging, and interpretation at multiple scales," Electroencephalography and clinical

Neurophysiology, vol. 103, no. 5, pp. 499-515, Nov. 1997, doi: 0.1016/s0013-4694(97)00066-7

[30] G. Nolte, O. Bai, L. Wheaton, Z. Mari, S. Vorbach, and M. Hallett, "Identifying true brain interaction from EEG data using the imaginary part of coherency," Clinical Neurophysiology, vol. 115, no. 10, pp. 2292-2307, Oct. 2004, doi: 10.1016/j.clinph.2004.04.029

[31] J. Lacaux, E. Rodriguez, J. Martinerie, and F. Varela, "Measuring phase synchrony in brain signals," Human Brain Mapping, vol. 8, no. 4, pp. 194-208, May 1999, doi: 10.1002/(sici)1097-0193(1999)8:4<194::aid-hbm4>3.0.co;2-c.

[32] R. Bruna, F. Maestu, and E. Pereda, "Phase locking value revisited: teaching new tricks to an old dog," Journal of Neural Engineering, vol. 15, no. 5, Oct. 2018, doi: 10.1088/1741-2552/aacfe4

[33] S. Aydore, D. Pantazis, and R. Leahy, "A note on the phase locking value and its properties," vol. 74, pp. 231-244, Jul. 2013, doi: 10.1016/j.neuroimage.2013.02.008

[34] M. Vinck, R. Oostenveld, M. Wingerden, F. Battaglia, and C. Pennartz, "An improved index of phase-synchronization for electrophysiological data in the presence of volume-conduction, noise and sample-size bias," Neuroimage, vol. 55, no. 4, pp. 1548-1565, Apr. 2011, doi: 10.1016/j.neuroimage.2011.01.055

[35] S. Yin, Y. Liu, and M. Ding, “Amplitude of sensorimotor mu rhythm is correlated with BOLD from multiple brain regions: a simultaneous EEG-fMRI study,” Frontiers in Human Neuroscience, vol. 10, no. 364, July 2016, doi: 10.3389/fnhum.2016.00364

[36] F. Farina, D. Emek-Savas, L. Rueda-Delgado, R. Boyle, H. Kiiski, G. Yener, and R. Whelen, "A comparison of resting state EEG and structural MRI for classifying Alzheimer's

disease and mild cognitive impairment," NeuroImage, vol. 215, July 2020, doi: 10.1016/j.neuroimage.2020.116795

[37] G. Knyazev, "Motivation, emotion, and their inhibitory control mirrored in brain oscillations," Neuroscience & Biobehavioral Reviews, vol. 31, no. 3, pp. 377-395, 2007, doi: 10.1016/j.neubiorev.2006.10.004

[38] M. Gola, M. Magnuski, I. Szumska, and A. Wrobel, "EEG beta band activity is related to attention and attentional deficits in the visual performance of elderly subjects," International Journal of Psychophysiology, vol. 89, no. 3, pp. 334-341, Sep. 2013, doi: 10.1016/j.ijpsycho.2013.05.007

[39] C. Tallon-Baudry, and O. Bertrand, "Oscillatory gamma activity in humans and its role in object representation," Trends in Cognitive Sciences, vol. 3, no. 4, pp. 151-162, Apr. 1999, doi: 10.1016/S1364-6613(99)01299-1

[39] C. Briels, D. Schoonhoven, C. Stam, H. de Waal, P. Scheltens, and A. Gouw, "Reproducibility of EEG functional connectivity in Alzheimer's disease," Alzheimer's Research and Therapy, vol. 12, no. 68, June 2020, doi: 10.1186/s13195-020-00632-3

[40] S. Kasakawa, T. Yamanishi, T. Takahashi, K. Ueno, M. Kikuchi, and H. Nishimura, "Approaches of Phase Lag Index to EEG Signals in Alzheimer's Disease from Complex Network Analysis," Innovation in Medicine and Healthcare, Smart Innovation, Systems, and Technologies, vol. 45, pp. 459-468, Aug. 2015, doi: 10.1007/978-3-319-23024-5_42

[41] T. Koenig, L. Prichep, T. Dierks, D. Hubl, L. Wahlund, E. John, and V. Jelic, "Decreased EEG synchronization in Alzheimer's disease and mild cognitive impairment," Neurobiology of Aging, vol. 26, no. 2, pp. 165-171, Feb. 2005, doi: 10.1016/j.neurobiolaging.2004.03.008

[42] C. Stam, A. van Walsum, Y. Pijnenburg, H. Berendse, J. de Munck, P. Scheltens, and B. van Dijk, "Generalized synchronization of MEG recordings in Alzheimer's Disease: evidence for involvement of the gamma band," Journal of Clinical Neurophysiology, vol. 19, no. 6, pp. 562-574, Dec. 2002, doi: 10.1097/00004691-200212000-00010

[43] J. van Deursen, E. Vuurman, F. Verhey, V. van Kranen-Mastenbroek, and W. Riedel, "Increased EEG gamma band activity in Alzheimer's disease and mild cognitive impairment," Journal of Neural Transmission, vol. 115, no. 9, pp. 1301-1311, July 2008, doi: 10.1007/s00702-008-0083-y

[44] D. Moretti et. al, "Individual analysis of EEG frequency and band power in mild Alzheimer's disease," Clinical Neurophysiology, vol. 115, no. 2, pp. 299-308, Feb. 2004, doi: 10.1016/s1388-2457(03)00345-6

[45] D. Moretti, D. Paternico, G. Binetti, O. Zanetti, and G. Frisoni, "EEG upper/low alpha frequency power ratio relates to temporo-parietal brain atrophy and memory performances in mild cognitive impairment," Frontiers in Aging Neuroscience, vol. 5, no. 63, Oct. 2013, doi: 10.3389/fnagi.2013.00063

[46] M. Cohen, "A better way to define and describe Morlet wavelets for time-frequency analysis," NeuroImage, vol. 199, pp. 81-86, Oct. 2019, doi:10.1016/j.neuroimage.2019.05.048

[47] C. Machado et al., "QEEG spectral and coherence assessment of autistic children in three different experimental conditions," Journal of Autism and Developmental Disorders, vol. 45, no. 2, pp. 406-424, Feb. 2015, doi: 10.1007/s10803-013-1909-5

[48] M. Vaziri-Pashkam, and Y. Xu, “Goal-directed visual processing differentially impacts human ventral and dorsal visual representations,” The Journal of Neuroscience, vol. 37, no. 36, pp. 8767-8782, Sep. 2017, doi: 10.1523/JNEUROSCI.3392-16.2017

[49] L. Sinclair, A. Kumar, T. Darreh-Shori, and S. Love, “Visual hallucinations in Alzheimer's disease do not seem to be associated with chronic hypoperfusion of to visual processing areas V2 and V3 but may be associated with reduced cholinergic input to these areas,” Alzheimer’s Research and Therapy, vol. 11, Sep. 2019, doi: 10.1186/s13195-019-0519-7

Appendix A: Sample MoCA Test

MONTREAL COGNITIVE ASSESSMENT (MOCA)
Version 7.1 Original Version

NAME :
Education : Date of birth :
Sex : DATE :

VISUOSPATIAL / EXECUTIVE — POINTS

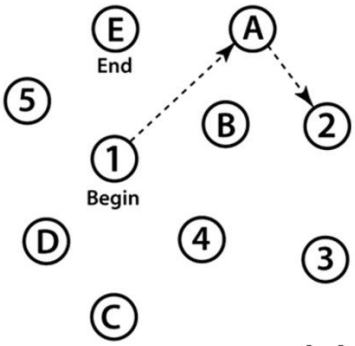

Copy cube

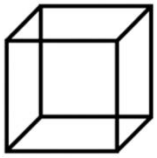

[ ] [ ]

Draw CLOCK (Ten past eleven)
(3 points)

[ ] Contour [ ] Numbers [ ] Hands

__/5

NAMING

[ ]

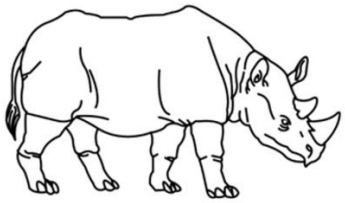

[ ]

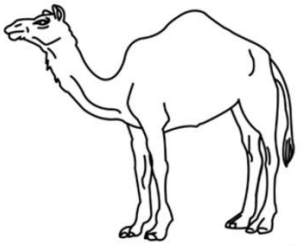

[ ]

__/3

MEMORY Read list of words, subject must repeat them. Do 2 trials, even if 1st trial is successful. Do a recall after 5 minutes.

	FACE	VELVET	CHURCH	DAISY	RED
1st trial					
2nd trial					

No points

ATTENTION Read list of digits (1 digit/ sec.).

Subject has to repeat them in the forward order [ ] 2 1 8 5 4
Subject has to repeat them in the backward order [ ] 7 4 2

__/2

Read list of letters. The subject must tap with his hand at each letter A. No points if ≥ 2 errors

[ ] F B A C M N A A J K L B A F A K D E A A A J A M O F A A B

__/1

Serial 7 subtraction starting at 100 [ ] 93 [ ] 86 [ ] 79 [ ] 72 [ ] 65

4 or 5 correct subtractions: **3 pts**, 2 or 3 correct: **2 pts**, 1 correct: **1 pt**, 0 correct: **0 pt**

__/3

LANGUAGE Repeat : I only know that John is the one to help today. [ ]
The cat always hid under the couch when dogs were in the room. [ ]

__/2

Fluency / Name maximum number of words in one minute that begin with the letter F [ ] _____ (N ≥ 11 words)

__/1

ABSTRACTION Similarity between e.g. banana - orange = fruit [ ] train – bicycle [ ] watch - ruler

__/2

DELAYED RECALL

	Has to recall words **WITH NO CUE**	FACE [ ]	VELVET [ ]	CHURCH [ ]	DAISY [ ]	RED [ ]	Points for UNCUED recall only
Optional	Category cue						
	Multiple choice cue						

__/5

ORIENTATION [ ] Date [ ] Month [ ] Year [ ] Day [ ] Place [ ] City

__/6

www.mocatest.org

Normal ≥ 26 / 30

TOTAL __/30

Add 1 point if ≤ 12 yr edu

Administered by: _____

Appendix B: IRB Approval

EAST CAROLINA UNIVERSITY
University & Medical Center Institutional Review Board
4N-64 Brody Medical Sciences Building· Mail Stop 682
600 Moye Boulevard · Greenville, NC 27834
Office **252-744-2914** · Fax **252-744-2284** ·
rede.ecu.edu/umcirb/

Notification of Amendment Approval

From: Social/Behavioral IRB
To: Sunghan Kim
CC:

Sunghan Kim
Date: 11/19/2021
Re: Ame5 UMCIRB 16-001636
UMCIRB 16-001636
Validating Event-Related Potential Tomography in Older Adults

Your Amendment has been reviewed and approved using expedited review for the period of 11/18/2021 to 9/15/2022. It was the determination of the UMCIRB Chairperson (or designee) that this revision does not impact the overall risk/benefit ratio of the study and is appropriate for the population and procedures proposed.

Please note that any further changes to this approved research may not be initiated without UMCIRB review except when necessary to eliminate an apparent immediate hazard to the participant. All unanticipated problems involving risks to participants and others must be promptly reported to the UMCIRB. A continuing or final review must be submitted to the UMCIRB prior to the date of study expiration.The investigator must adhere to all reporting requirements for this study.

Approved consent documents with the IRB approval date stamped on the document should be used to consent participants (consent documents with the IRB approval date stamp are found under the Documents tab in the study workspace).

The approval includes the following items:

Document	Description
Lana Wang being added to the study	

For research studies where a waiver or alteration of HIPAA Authorization has been approved, the IRB states that each of the waiver criteria in 45 CFR 164.512(i)(1)(i)(A) and (2)(i) through (v) have been met. Additionally, the elements of PHI to be collected as described in items 1 and 2 of the Application for Waiver of Authorization have been determined to be the minimal necessary for the specified research.

The Chairperson (or designee) does not have a potential for conflict of interest on this study.
